THE BEGINNING OF BEDLOAD MOVEMENT OF MIXTURES INVESTIGATED AS NATURAL ARMORING IN CHANNELS

by

Johannes Gessler
Dr. sc. techn.
(1965)

Translated with permission of the Author and
The Swiss Federal Institute of Technology
by Edmund A. Prych

at

W. M. Keck Laboratory of Hydraulics and Water Resources
Division of Engineering and Applied Science
California Institute of Technology
Pasadena, California

March 1967
Revised October 1968

THE BEGINNING OF BEDLOAD MOVEMENT OF MIXTURES INVESTIGATED AS NATURAL ARMORING IN CHANNELS

by

Johannes Gessler

Dr. sc. techn.

(1965)

Report No. 69 of the Laboratory of Hydraulic Research and Soil Mechanics of the Swiss Federal Institute of Technology in Zurich under the direction of Prof. G. Schnitter.

Translated with permission of the Author and
The Swiss Federal Institute of Technology
by Edmund A. Prych

at

W. M. Keck Laboratory of Hydraulics and Water Resources
Division of Engineering and Applied Science
California Institute of Technology
Pasadena, California

Reproduction of this material was sponsored
under a grant from the Bechtel Corp.

FOREWORD 3*

In this paper the beginning of bedload movement of mixtures is investigated.

I wish to express my sincere thanks to Prof. G. Schnitter, my advisor, for the expert guidance and valuable suggestions which contributed to the success of this work. I thank Prof. Th. Dracos for reviewing and approving the work, in this way he assisted in this project. I thank Engineer J. Zeller, Chief of the Department of Hydraulics in the Laboratories of Hydraulic Research and Soil Mechanics of the Swiss Federal Institute of Technology, for the great interest and the assistance that he provided for this work at many times. To Mr. J. Zeller, draftsman, I give my thanks for the careful preparation of all drawings and writing the equations. Furthermore, I wish to thank every employee of the Laboratories of Hydraulic Research and Soil Mechanics, that assisted me many times with advice and actions, especially while conducting the experiments.

Johannes Gessler

Itschnach-Kusnacht, December 1965

---

* Underlined numbers in the right hand margin are page numbers in the original text.

CONTENTS

Page

SUMMARY 5

SUMMARY 7

LIST OF SYMBOLS 8

INTRODUCTION 12

1. THE BEGINNING OF BEDLOAD MOVEMENT 14

1.1 Incipient Motion of a Single Grain According to Shields 14

1.2 The Beginning of Bedload Movement of Mixtures 17

1.3 Fundamental Remarks on the Definition and Experimental Determination of the Critical Shear Stress 22

1.4 Remarks on the Experimental Determination of the Critical Shear Stress by Shields 23

2. EXPERIMENTAL DETERMINATION OF THE BEGINNING OF BEDLOAD MOVEMENT OF MIXTURES 32

2.1 The Process of Armoring as a Problem of the Beginning of Incipient Motion 32

2.2 The Armoring Experiments 35

2.3 Analysis of the Experimental Results 45

3. COMPARISON WITH FIELD MEASUREMENTS 65

3.1 The Aare River above Brienzer Lake 65

3.2 Irrigation Canal in the San Luis Valley, Colorado 68

CONTENTS (continued)

Page

4. SUGGESTED POSSIBILITIES FOR ADDITIONAL INVESTIGATIONS 70

4.1 Turbulence Measurements in the Proximity of a Rough Boundary 70

4.2 Investigations on the Necessary Amount of Erosion Required to Stabilize a Bed 71

4.3 Investigations on the Comparison of the Particle Size Distributions of the Moving Materials in Pure Armoring Experiments and in Experiments with Continuous Movement 74

5. APPENDIX 75

6. PHOTOGRAPHS 85

7. REFERENCES 89

SUMMARY

5

Beginning of bedload transport in channels, whose beds are formed by gravel-sand mixtures, is theoretically and experimentally investigated.

In order to make a theoretically approachable treatment to the problem two assumptions are made:

1. the turbulent fluctuations of the bottom shear stress are statistically describable by a Gaussian distribution;

2. a grain starts in motion when the effective (instantaneous) eroding bottom shear stress on a grain exceeds a critical value, which is a function of the grain size and Reynolds number of the grain.

On the basis of these assumptions the probability of remaining still (or being eroded) for a certain grain under given hydraulic conditions is calculated (equation 8; this probability is independent of the grain size distribution of the gravel-sand mixture). During the work a feasible way was found to determine the critical shear stress by a basically new method: the average bottom shear stress was defined as equal to the control shear stress, when for the grain in question, the probability for remaining still and being eroded are equal.

To supplement and verify the theory, natural armoring of channel bottoms consisting of gravel-sand-mixtures was investigated in the laboratory. On the basis of these experiments the dimensionless critical shear stress can be determined as a function of the Reynolds number of the grains (Fig. 8), and the distribution function of the fluctuation of the bottom shear stress (Fig. 9); in doing so it was confirmed that the distribution function can be approximated by

the Gaussian distribution with a standard deviation of $\sigma = 0.57$.

The laboratory experiments were supplemented by observations in the field.

SUMMARY

In this investigation the beginning of motion is theoretically and experimentally studied on channel beds formed by noncohesive sediment mixtures with large grain size distribution curves.

To study this problem theoretically two assumptions are made:

1. the turbulent fluctuations of the bed shear stress are distributed according to the normal error law (equation 5);
2. motion of grain will occur when the effective momentary shear stress acting at the grain exceeds a critical value (equation 6), which is given by equation 7.

By combining these three equations the probability that the critical shear stress at a certain grain is not exceeded is calculated (equation 8). From equation 8 we get a very objective definition of the critical shear stress, which is given by equation 9. This definition is valid independent of any grain size distribution, unit grain sizes as well as sediment mixtures.

In order to check and complement the theory, the natural armoring of channel beds formed by sediment mixtures was studied in laboratory model tests. A channel bed formed by a sediment mixture was exposed to a constant mean bed shear stress. The erosion of the smaller grains is now more probable than the erosion of the larger ones. Gradually these larger grains will form a stable top layer, one grain thick, which prevents the underlying sediment mixture from any further erosion. Thereby each grain, depending on whether it is eroded or stays as an ingredient of the top layer, may be taken as an indicator of whether or not the critical shear stress at this grain is exceeded. Taking a specific grain size and the corresponding critical shear stress, the probability that the critical shear stress is not exceeded is given by the ratio between the number of grains of this specific size which stay in the top layer and the total number of grains of this size which were exposed to the fluid. This probability is the same as that formulated in equation 8.

By measuring in the model test the gradient of the energy line and the depth and the discharge of water, it is possible to calculate the mean bed shear stress, taking into account the wall effect (equations 13, 18, 19, 20, 23). By measuring the grain size distribution curves of the underlying material, the top layer, and the eroded material as well as by measuring the weight per unit bed area of the top layer and the eroded material, it is possible to calculate the probability for each grain size of staying as an ingredient of the top layer with equations 25, 30 or 37 (figure 11). The dimensionless critical shear stress T_c is calculated with equation 39 (figures 11 and 8). As soon as T_c is known for each grain size, it is possible to calculate the statistical distribution of the shear stress fluctuations with equation 40 (figure 9).

The laboratory model test results were complemented by measurements made in nature in a 7
river (Aare) with water discharges between 3300 and 7600 cubic feet per second as well as in irrigation channels in the San Luis Valley, Colorado. The measurements made in the Aare River show very good agreement with the model test results (figure 9) whereas the measurements in the San Luis Valley show a considerable error between theory and measurements (figure 10). This discrepancy, however, is the result of incorrect grain size distribution curves of the top layer materials, as the finer grains are missing from these curves.

Photograph 1 is a cross section of a stable armored channel bed, and photographs 2 to 5 show the different phases during the development of such a stable top layer. In photograph 6 colophony is poured on the bed in order to remove the top layer as soon as the colophony is hardened again. In photograph 7 the top layer is removed. Photograph 8 shows the top layer from below. (The photographs 2 to 8 show always the same section of the bed during one test run.)

LIST OF SYMBOLS

A_f	grain shape factor (cross sectional area factor)
A_v	grain shape factor (volume factor)
a	dynamic uplift
b	channel width
f	cross sectional area of the flow
f_e	cross sectional area of a single grain
Δf	total cross sectional areas of the single grains
g	acceleration due to gravity = 9.81 m/sec^2
g	(with index) weight per unit surface area of sand-gravel-mixture
h	depth of flow
J	energy slope
k	grain size
k_m	average grain size of a gravel-sand-mixture
k_{max}	maximum grain size of a gravel-sand-mixture
K	dimensionless grain size
$\overline{m}$	controlling average bottom shear stress for bedload movement
s	number of grains per unit surface area in the armor layer
p	wetted perimeter
Δp	relative weight of asize-fraction of a gravel-sand-mixture (as a fraction of one)
q	probability of not exceeding the critical shear stress; i.e. probability of remaining still.

Q	water discharge through the total channel cross-section
r	hydraulic radius
Re	Reynolds number
Re_*	Reynolds number of the grain
T	dimensionless bottom shear stress
T_c	dimensionless critical shear stress
u	velocity
u_*	shear velocity
w	fall velocity
y	distance from the boundary
γ_s	specific weight of the grains
γ_w	specific weight of the fluid
δ_l	thickness of the laminar sub-layer
λ	coefficient of roughness 9
ν	kinematic viscosity
π	3.14 ...
ρ_w	density of the fluid
σ	standard deviation of the Gaussian distribution
τ	effective bottom shear stress
τ_c	critical shear stress

INDICES

A	starting mixture
D	top layer mixture
E	eroded mixture

i, j	number of grain fraction
k	grain
s	bottom
w	side-wall

A quantity with an overbar is a time averaged value.

INTRODUCTION

The river-and channel-bottoms of streams conveying water through alluvium show the tendency to be armored with the larger components of the alluvium. A closer study of this phenomenon shows that the top layer is not only made of these larger components which certainly are predominant, but rather that in the top layer also all the smaller grains which are present in the underlying mixture. Therefore, during the armoring process a selective process occurs during which the erosion of the finer fraction is preferred and consequently the larger components are concentrated in the top layer of the bed, but there is no distinct boundary created between the erodable and nonerodable grain sizes.

These facts suggest treating this selection process with probability theory. The larger the grain the less is the probability that it will erode, or the larger the probability that it will remain as a part of the armoring.

The grain goes from rest to a state of motion when the instantaneous local bottom shear stress on the grain exceeds a criticial value that is dependent on the grain diameter; therefore it is possible to combine the theoretical probability treatment of the selection process with a statistical interpretation of the turbulent fluctuations of the bottom shear stress.

In the first chapter, after a short introduction to the problem of the controlling shear stress, a new theory is given that combines both the selection process and trubulent fluctuations of the bottom shear stress. In the second chapter the results of the theoretical investigation are verified by laboratory experiments, and in the third chapter comparisons with field observations are found.

In the fourth chapter some problems are proposed that were only touched on in this work and were not treated in detail, which if carried out could yield a valuable supplement.

In the appendix follow sample calculations for the evaluation of test results, for the comparison of theory and laboratory experiment, and theory and field observations.

1. THE BEGINNING OF BEDLOAD MOVEMENT

1.1. Incipient Motion of Uniformly Sized Grains According to Shields

The beginning of bedload movement in straight channels with two-dimensional flow was the sybject of numerous investigations during the past decades. Briefly it is the following problem:

A flat bed of a channel is made of loose grains. Over this flat bed moves a current that exerts a certain shear stress on the channel bottom. When the shear stress exceeds a critical value, the forces acting on an individual grain become large enough so that the effective weight of the grain is overcome and the grain moves from its position of rest.
The investigation concerning this process had the general aim of finding the relationship between the grain size and critical shear stress.

The basic work on this problem was published by Shields (17) in 1936. He put the results of his theoretical and experimental investigation into the following proposition:

"The ratio of the active force of the water parallel to the bed, to the resistance of a grain on the bed is a unviersal function of the ratio of the grain size to the thickness of the laminar sublayer."

Therefore, according to Shields:

$$\frac{\tau_o}{(\gamma_s - \gamma_w)k} = f_1 \cdot \left(\frac{k}{\delta_1}\right) = f_2 \left(\frac{u_* k}{\nu}\right) \qquad (1)$$

τ_c critical shear stress

γ_s specific weight of the grain

γ_w	specific weight of the fluid
k	grain size
δ_1	thickness of the laminar sublayer
ν	kinematic viscosity
u_*	shear velocity
ρ_w	density of fluid
τ	bottom shear stress

$$u_* = \sqrt{\frac{\tau}{\rho_w}}$$

Shields determined the functions f_1 and f_2 by experimental methods for the case in which the grains that form the bed are uniform in size. During the course of the experiments the difficult question of the definition of incipient motion arose; due to various reasons the uniform size grains did not all begin to move at the same time. Shields defined the beginning of motion in the following way: he found in experiments with different bottom shear stresses, that were just above critical, small bedload transport rates per unit time. He extrapolated the function for bedload movement dependent on bottom shear stress obtained in this way in the direction of decreasing bottom shear stress to the point where the bedload transport is zero. He called the corresponding shear stress of this point the "critical shear stress". For the condition that the bed is made of grains of uniform size, the validity of the relation found by Shields is almost generally accepted.

The Japanese, Iwagaki (8), tried to theoretically derive the Shields function. Without going into the complicated mathematical problems of the derivation, it is pointed out that in general Iwagaki found good agreement with Shields' observations.

Liu (13) used an interesting modification of the Shields function; in it he replaced the value $\frac{\tau_c}{(\gamma_s - \gamma_w)k}$ by the ratio $\frac{u_{*c}}{w}$ where $u_{*c} = \sqrt{\frac{\tau_c}{\rho_w}}$ is the critical shear velocity and w is the fall velocity in still water. In principle the function is equivalent to that by Shields, in that both the new variables introduced are clearly functions of τ_c and k respectively. The advantage of the development by Liu is that the fall velocity is to a certain degree dependent on the grain shape. But this advantage at once undergoes a limitation in that, in general, during the falling process the shortest axes of the grains are parallel to the direction of fall, while in the problem of the beginning of bedload movement the grains are lying on the bed, and therefore, the shortest axes are mostly normal to the flow velocity.

The usability of the Shields function in practice is limited; the function was determined for the case in which the bed is made of purely equal size grains. Shields indeed tried to extend his investigation to the case where the bed consists of a mixture of different size grains. He relied on the investigations of Casey (1) and Kramer (11), who introcuced a controlling grain diameter and a non-uniformity constant for the mixture. However, at best, this succeeded only when one used bottom shear stresses in connection with bedload transport studies considerably above the critical shear stress. The calculation of the critical shear stress for a bed that consists of a mixture of different size grains (each grain size has a different critical shear stress, as equation (1) shows) cannot be accomplished by the Shields method. However, this topic shall be 14
the subject of this report, because the phenomena of natural armoring or the phenomena of partial bedload movement, as described by e. g. Nizery and Brandeau (15), occurs just in the range of relatively small shear stresses.

Furthermore Shields function has the considerable disadvantage that it was not measured directly, but had to be extrapolated in turn from a number of plotted points. As a consequence, this indirect procedure resulted in numerous possibilities for inaccuracies (measurement errors, difficulties in extrapolation), leading to a considerable scattering of the points determined by Shields. Therefore, Shields gave up on obtaining a curve $T_c = f(Re_*)$, the definite boundary between sub- and supercritical bottom shear stress.

1.2. The Beginning of Bedload Movement of Mixtures

In this section an attempt will be made to formulate a theory for the beginning of bedload movement for the case in which the bed consists of a mixture of different size grains, which in natural water courses as well as in man-made channels is mostly the case.

Einstein and El Samni (6) showed that the dynamic uplift on a single grain subjected to turbulent fluctuations is statistically distributed according to the Gaussian distribution. The average dynamic uplift (per unit area) is

$$\bar{a} = C_L \cdot \rho_w \cdot \frac{\bar{u}^2}{2} \qquad (2)$$

$\bar{a}$	average dynamic uplift
C_L	constant
$\bar{u}$	average velocity at a theoretical distance from the boundary 0.35 k

In order to find the relationship between the average dynamic uplift and average bottom shear stress, the velocity in equation (2) is calculated with the aid of the logarithmic velocity distribution for open channels with rough boundaries (see e.g. Keulegan (10), Schlichting (16)).

$$\frac{\overline{u}}{u_*} = 8.5 + 5.75 \log \frac{y}{k} \qquad (3)$$

$\overline{u}$ average velocity at a distance from the boundary y 15

y distance from the boundary

With $y = 0.35\, k$ one obtains for $\overline{u}$

$$\overline{u} = 5.9\, u_*$$

One recalls that $u_* = \sqrt{\overline{\tau}/\rho_w}$, so one obtains

$$\overline{u}^2 = 34.8 \frac{\overline{\tau}}{\rho_w}$$

$\overline{\tau}$ average bottom shear stress

One introduces this expression into equation (2), so one sees that the average dynamic uplift is directly proportional to the bottom shear stress

$$\overline{a} = 17.4 \cdot C_L \cdot \overline{\tau} \qquad (4)$$

Einstein and El Samni stated that for the case when a half a sphere is used in place of a grain, $C_L = 0.178^*$.

When the dynamic uplift on a single grain is distributed according to the Gaussian distribution the same is also true for the bottom shear stress. One defines the absolute fluctuation of the bottom shear stress $\tau - \overline{\tau} = \tau'$, where $\overline{\tau}$ is the average bottom shear stress; the probability for τ' being smaller than a value t is

$$W(\tau' < t) = \frac{1}{\sigma\sqrt{2\pi}} \int_{-\infty}^{t} e^{-\frac{x^2}{2\sigma^2}} \, dx \qquad (5)$$ 16

σ standard deviation of the Gaussian distribution

x dummy variable of integration

In order to change over from the statistical distribution of shear stress to the problem of the beginning of bedload movement one assumes that a grain is eroded when

$$T = \frac{\tau}{(\gamma_s - \gamma_w)k} > T_c \qquad (6)$$

T dimensionless shear stress

Analogous to equation (1), T_c is a function of the Reynolds number of the grain

---

*It is pointed out that C_L can hardly be called a constant, but is a function of the Reynolds number of the grain. This dependence is very weak in the turbulent region, where in nature it normally exists, so that the fluctuation of the Reynolds number due to turbulence only slightly influences the value of C_L.

$$T_c = \frac{\tau_c}{(\gamma_s - \gamma_w)k} = f\left(\frac{u_* k}{\nu}\right) \qquad (7)$$

Now, to be sure, condition (6) applies to single grains, and the controlling momentary effective bottom shear stress, τ. For a given grain size (with a given kinematic viscosity) T_c is a constant in the sense that it is independent of the turbulent fluctuations (see also Fig. 1). The probability for the critical shear stress not to be exceeded for a single grain is calculated from equation (5), in which the value $\tau_c - \bar{\tau}$ is inserted for t. One obtains τ_c from equation (7). The corresponding relative value $\frac{\tau'}{\bar{\tau}}$ is introduced for the absolute value of τ'.

$$q = W\left(\frac{\tau'}{\bar{\tau}} < T_c \frac{(\gamma_s - \gamma_w)k}{\bar{\tau}} - 1\right) = \frac{1}{\sigma\sqrt{2\pi}} \int_{-\infty}^{T_c \frac{(\gamma_s - \gamma_w)k}{\bar{\tau}} - 1} \exp\left[-\frac{x^2}{2G^2}\right] dx \qquad (8)$$

q probability of the critical shear stress not being exceeded, or probability of a grain remaining stationary.

Therefore q is a function of $\bar{\tau}/(\gamma_s - \gamma_w)k$, T_c, and σ. According to equation (7), T_c is a function of the Reynolds number of the grain. Einstein (7) said that σ is a universal constant. Even if it should be shown that this is not true, it is likely that above all it is a function of the Reynolds number of the controlling grains (most likely for the mixtures in question, the maximum grain size). 17

This is because σ is a convenient way of describing the turbulence in the proximity of the bed and therefore is a function of the local average velocity, the size of the roughness elements, and the kinematic viscosity of the fluid.

Equation (8) can be written generally as

$$q = \left(\frac{\overline{\tau}}{(\gamma_s - \gamma_w)k}, \frac{u_* k}{\nu}\right) = f\,(\overline{T}, Re_*)$$

as long as one assumes with Einstein that σ is a constant.

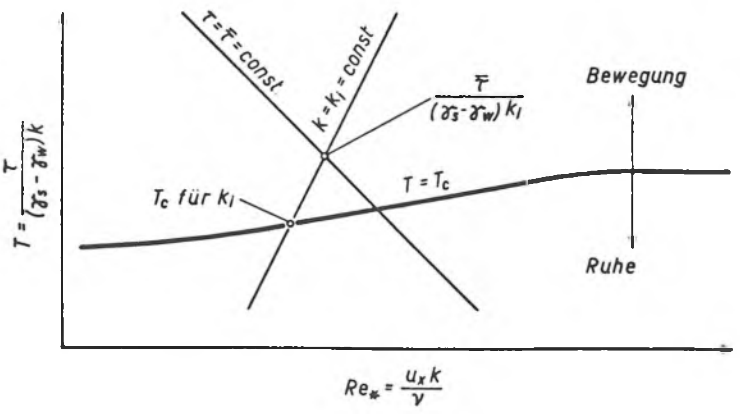

Figure 1. T-Re_* Diagram. For a given average bottom shear stress $\overline{\tau}$ the different grain sizes of the gravel-sand-mixture lie along the straight line $\tau = \overline{\tau}$ = constant. Due to the turbulent fluctuation of τ the point corresponding to the grain size k_i fluctuates on the straight line $k = k_i$ = constant with the average at $\frac{\overline{\tau}}{(\gamma_s - \gamma_w)k}$. The curve $T = T_c$ forms the boundary between movement and rest.

1.3. Comments on the Definition and Experimental Determination of the Critical Shear Stress

In all the literature suggesting methods for the determination of the critical shear stress the methods are based on the assumption that when the average shear stress is equal to the critical that this instant can be determined in some way, e.g. by purely visual methods 18 in the experiment observing when the first grain begins to move; or (as Shields assumed) at $\overline{\tau} \leq \tau_c$ that bedload movement stops.

For basic reasons it is not possible to determine visually that instant when $\tau_c = \tau$; due to turbulence individual grains are moved when the average shear stress is less than critical. This fact (while not always the cause) is usually recognized. Therefore, one is helped by an arbitrary method in which, for example, $\tau_c = \overline{\tau}$ is defined for the case when one determines that an arbitrarily selected number of grains per unit surface are in motion. On the other hand Yalin (20) pointed out the defects of this kind of definition and the general difficulties of the definition and experimental determination of the critical shear stress, but without offering an alternative.

This determination method by Shields (see Section 1. 1) is certainly superior to these visual methods, since he defined the critical shear stress on a physical basis. But Yalin (20) points out certain difficulties occuring from the extrapolation of the bedload movement function. In the following section, 1. 4, these difficulties and their causes are investigated in detail.

In contrast, equation (8) shows the possibility of defining exactly the critical shear stress, indicating the exact moment that the average shear stress is equal to the critical. One puts into equation (8) $\tau_c = \overline{\tau}$, the upper limit of the integral is equal to zero and the probability of remaining still is equal to 0.5 and is independent of the standard deviation.

$$\tau_c(k) = \overline{\tau}$$
$$q\ (k) = 0.5 \qquad (9)$$

The average bottom shear stress is therefore equal to the critical for a particular grain when the probability of eroding is equal to the probability of remaining still. This definition is independent of whether the bed consists of a mixture of different size grains, or it is made (as in the case of Shields) of uniform grains.

In the next chapter a possible method is proposed to determine experimentally, from an objective viewpoint, the probability of remaining still, and from it the critical shear stress.

1.4. Remarks on the Experimental Determination of the Critical Shear Stress by Shields 19

Shields had used the most objective method of determining the critical shear stress; therefore his experiments will be discussed here in more detail. There are two basic objections to make against his method whose influences on the value of the critical shear stress found will be discussed.

(1) Influence of turbulence on bedload transport for shear stresses close to the critical shear shear stress

Shields conducted his investigation exclusively with the use of average values. Because in this study turbulence is especially significant, the influence of the turbulent fluctuations of the bottom shear stress on the practicality of determining the critical shear stress according to the Shields method is investigated more precisely.

Shields started from the assumption that the amount of bedload movement is controlled by the difference between the average bottom shear stress and the critical shear stress. One must bear in mind that the bottom shear stress is fluctuating, so one must say more exactly, that the difference between the effective (instantaneous) and critical shear stress is to be considered as controlling the amount of movement. The time average of this difference is the control for the time average of the bedload movement. The difference is that Shields first averaged the bottom shear stress and then took the difference between this average and the critical shear stress, while here the difference between the effective bottom shear stress and critical shear stress is taken first and then this difference is averaged over time.

As long as the effective bottom shear stress always remains higher than the critical, both methods give the same value for the difference and the average value of the difference. However, if the average bottom shear stress is only a relatively small amount larger than the critical, then the effective shear stress sometimes goes below the critical, i.e. the difference is sometimes negative. Then the controlling difference for the bedload movement is to be sure zero, regardless of the absolute value of the negative difference; then it is insignificant for the grain as to how much the effective shear stress is below the critical shear stress; it is significant only in that it is below and that there is no movement. When one forms the average value of the controlling difference for the bed load transport one obtains a value larger than determined by Shields' method. (See Fig. 2.) Especially for $\overline{\tau} = \tau_c$ the bed load transport ceases according to Shields, which is not true; in this case the critical shear stress is exceeded 50% of the time and therefore bedload transport occurs.

20

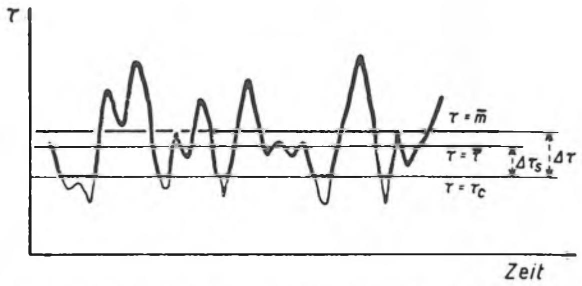

Δτ für den Geschiebetrieb effektiv massgebende Differenz
Δτs für den Geschiebetrieb massgebende Differenz nach Shields

$\Delta\tau$ for bedload movement, effective controlling difference
$\Delta\tau_s$ for bedload movement, controlling difference according to Shields.

Figure 2. Effective bottom shear stress as a function of time.

With the assumptions that the fluctuations of the bottom shear stress is described statistically by the Gaussian distribution and the standard deviation σ is known, the difference between the two methods can be calculated. The average value of the shear stress lying above the critical is

$$\overline{m}' = \frac{1}{\sigma\sqrt{2\pi}} \int_{\tau_c}^{+\infty} \tau \cdot e^{-\frac{(\tau-\overline{\tau})^2}{2\sigma^2}} \, d\tau \qquad (10)$$

One makes the substitution $X = \frac{\tau - \overline{\tau}}{\sigma}$, simplifying equation (10)

$$\overline{m}' = \frac{1}{\sqrt{2\pi}} \int_{X_c}^{+\infty} (\sigma X + \overline{\tau})\, e^{-\frac{X^2}{2}}\, dX \qquad X_c = \frac{\tau_c - \overline{\tau}}{\sigma}$$

The first part of this integral is easily integrated 21

$$\overline{m}' = \frac{\sigma}{\sqrt{2\pi}}\, e^{-\frac{X_c^{\,2}}{2}} + \overline{\tau}\, \frac{1}{\sqrt{2\pi}} \int_{X_c}^{+\infty} e^{-\frac{X^2}{2}}\, dX \qquad (11)$$

One bears in mind that as long as $\tau < \tau_c$ the controlling difference for the bedload transport is zero, i.e. the controlling bottom shear stress is equal to τ_c, therefore the controlling average bottom shear stress for the bedload transport is calculated as

$$\overline{m} = \overline{m}' + \tau_c \frac{1}{\sqrt{2\pi}} \int_{-\infty}^{X_c} e^{-\frac{X^2}{2}}\, dX$$

One inserts for $\overline{m}'$ the value from equation (11) and obtains $\overline{m}$ with respect to the average bottom shear stress $\overline{\tau}$ which gives

$$\frac{\overline{m}}{\overline{\tau}} = \frac{\sigma}{\overline{\tau}} \frac{1}{\sqrt{2\pi}} e^{-\frac{X_c^2}{2}} + \frac{\tau_c}{\overline{\tau}} + \left(1 - \frac{\tau_c}{\overline{\tau}}\right) \frac{1}{\sqrt{2\pi}} \int_{X_c}^{+\infty} e^{-\frac{X^2}{2}} dX \quad (12)$$

An evaluation of equation (12) is given in table 1 where the average bottom shear stress $\overline{\tau}$ and the controlling average bottom shear stress $\overline{m}$ are compared with one another for different ratios of $\frac{\overline{\tau}}{\tau_c}$. (See also Fig. 3.) The value $\frac{\sigma}{\overline{\tau}} = 0.57$ was used for the standard deviation (as will be shown later to be a reasonable value).

$\frac{\overline{\tau}}{\tau_c}$	$\frac{\overline{m}}{\tau_c}$	$\frac{\overline{m}}{\overline{\tau}}$
4.00	4.100	1.025
3.00	3.102	1.034
2.00	2.120	1.060
1.50	1.648	1.099
1.00	1.227	1.227
0.50	1.005	2.009

Table 1

If one plots the magnitude of the bedload transport as a function of $\overline{\tau}$, this curve would not yield a value of zero at $\overline{\tau} = \tau_c$. From table 1 one sees that for this case the deviation of $\overline{m}$ from $\overline{\tau}$ is only slightly more than 20%. For increasing values of $\overline{\tau}$ the error decreases quickly and at $\overline{\tau} = 1.5\ \tau_c$ it amounts to merely 10%. When one compares this systematic error with the scatter of the points measured by Shields, one realizes that Shields' simplification, to consider the controlling difference as being between $\overline{\tau}$ and τ_c, is permissible as long as $\overline{\tau} > 1.5\ \tau_c$, which for the majority of Shields' measured points is true. 22

Basically the question which presents itself is whether for these relatively high average bottom shear stresses, not $\overline{m}$, but rather $\overline{\tau}$ is the controlling value for bedload transport, because for the short time when the shear stress is less than τ_c the inertia of the grain prevents it from temporarily coming to rest. Therefore, systematic errors due to turbulence would not be produced in the measurements of Shields.

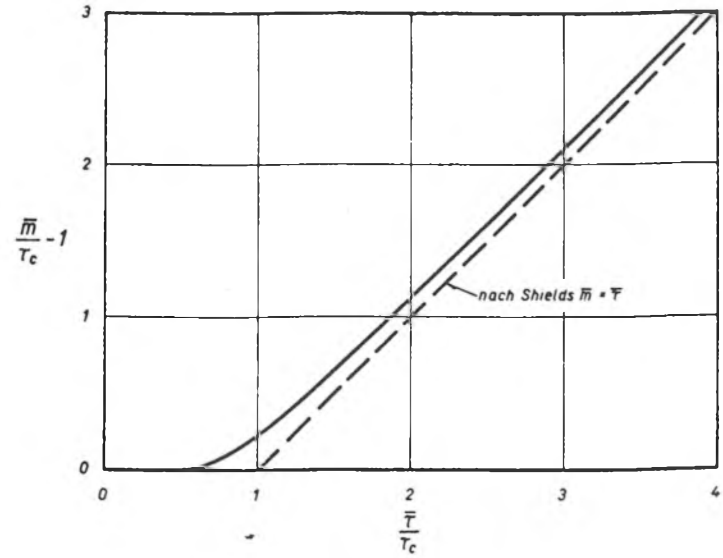

Figure 3. The controlling value $\frac{\overline{m}}{T_c} - 1$ for bed load transport as a function of $\frac{\overline{T}}{T_c}$ (see table 1).

(2) Influence of Bed Deformations on the Measurements of Shields

Shields determined the critical shear stress on the basis of measurements, which in part took place with an uneven bed (which Shields confirmed in his publication and is shown by a comparison of Shields measurements in a diagram by Liu (13)). This uneven bed creates an additional roughness element which consequently reduces the effective bottom shear stress on the grain. Because Shields did not recognize this influence it must be expected that he systematically obtained too large of values for the critical shear stress, which must result in his curve $T_c = f(Re_*)$ lying too high compared with the curve $q = 0.5$. An evaluation of the Shields diagram from this point of view shows that in the range $80 < Re_* < 400$ where Shields mentioned only "minor bed deformations" the observed points for sand follow closely a single line with only slight scatter. But for smaller Reynolds numbers where Shields mentioned "bars" and "ripples" the points seem to deviate systematically being about 10% too high. Because Shields gave the roughness coefficient for some of his measured points, that he observed during bedload transport, one can qualitatively estimate for these cases the probable influence of the bed deformations. From the stated values for λ_s and Re

$$\lambda_s = \frac{2\, r_s\, g\, J}{\bar{u}_m^2} \qquad\qquad Re = \frac{\bar{u}_m r_s}{\nu}$$

λ_s roughness coefficient

r_s hydraulic radius

J energy slope

$\bar{u}_m$ average velocity in the channel cross section

g acceleration due to gravity

The average velocity in the channel cross section and the controlling hydraulic radius can be calculated

$$\bar{u}_m = \sqrt{\frac{2\, Re\, \nu\, g\, J}{\lambda_s}} \qquad\qquad r_s = \frac{Re \cdot \nu}{\bar{u}_m}$$

The grain roughness λ_k is now given by (see e.g. Keulegan (10))

$$\lambda_k = \frac{1}{4}\left(2.21 + 2.03 \log \frac{r_s}{k}\right)^{-2} \quad * \qquad \underline{24}$$

---

*The factor $\frac{1}{4}$ is due to a difference in the definition of λ by Shields and by Keulegan.

The ratio $\frac{\lambda_k}{\lambda_s}$ now gives the factor to reduce the critical shear stress determined by Shields.

Unfortunately the measurements of λ by Shields were obviously not all carried out in conjunction with bedload measurements; namely serier of measurements of λ were considered in which no bedload transport occurred . Therefore, unfortunately some observations were not usable. While a usable measured point lies in the region of "minor bed deformations" gives a ratio $\frac{\lambda_k}{\lambda_s} = 1$ (as must be expected); the other measured points that lie in the region of bed unevenness must be reduced yielding a critical shear stress in the order of magnitude of about 10% lower. After carrying out the correction these measured points obtained on the basis of measurements in the region of "surface unevenness" also plotted on the curve as in the region of minor bed deformations.

This method to eliminate the influence of bed deformations in Shields' measurements, certainly includes considerable uncertainties. But the topic of the presented method is not to compute the real critical shear stress upon Shields' measurements but rather to evaluate the order of magnitude of the influence of bed deformations.

One sees that from the results of the theory developed here for the beginning of bedload transport in beds composed on non-uniform grain sizes, one can say that from knowledge of the function $T_c = f(Re_*)$ and the standard deviation σ of the statistical fluctuation of the shear stress, with the help of equation (8) the probability of not exceeding the critical shear stress (or no movement) for any grain under given hydraulic conditions can be calculated. The case of a bed of uniform grain size is a special case of this theory. As a guideline one may expect that the function $T_c = f(Re_*)$ lies about 10% lower than the average values measured by Shields, but otherwise shows an analogous shape. For the standard deviation σ Einstein used a value of $\sigma = 0.5$ in his bedload transport formula, which likewise may serve as a guideline.

More information on both values T_c and σ is given in the following chapters.

2. EXPERIMENTAL DETERMINATION OF THE BEGINNING OF BEDLOAD MOVEMENT OF MIXTURES 25

2.1 The Process of Armoring as a Problem of Incipient Bedload Movement.

In order to prove experimentally the theory for the beginning of bedload movement, the phenomena of the natural armoring of channel beds, composed of mixtures, was investigated in a model. The problem is concerned with the following process:

A plane bed is formed in a channel consisting of a homogeneous mixture of different size grains. A constant average bottom shear stress acts on this bed while a known discharge flows over it. As previously stated in the above chapter the erosion of the finer fraction of the mixture is more probable that the erosion of the coarse fractions. The removal of the finer fractions brings about the exposure of more larger components that can not be eroded, or of which erosion is at least very unlikely. These larger components gradually form a dense cover, an armor, a top layer, protecting the material lying underneath (the initial bed forming mixture) from further erosion with time. (Below the following names are used: the phenomena as such is called armoring; the top layer is the upper layer of grains on the bed that was exposed directly to the current but was not eroded; the material that forms the bed before the experiment is called the starting mixture, and consequently is found beneath the top layer; the eroded mixture is the material carried away and consequently sampled at the end of the flume; the top layer mixture is the material that forms the top layer).

The formation of an armor is therefore due to a fraction of the grains that are directly exposed to the current but for which the controlling critical shear stress of each grain is not exceeded. Each grain can therefore be used as an indicator for whether the critical shear stress for it was exceeded or not. One examines a certain size fraction of the grains and its associated critical shear stress; the ratio of the number of grains in this fraction which remained to the total number of grains in the fraction which were generally exposed to the current (therefore the sum of the grains remaining and those eroded) is equal to the probability that the corresponding critical shear stress was not exceeded; i.e. that probability which was formulated in a previous chapter as in equation (8).

When one has at his disposal a sufficient number of measurements of this ratio for different grain sizes and different average bottom shear stresses it is possible to determine the function $T_c = f(Re_*)$ and the standard deviation σ of the statistical distribution function.

Concerning the question, under what conditions the non- 26
moving grains form a stable top layer, is not gone into in detail here. The object of this investigation, primarily, is the beginning of bedload movement and not the phenomena of armoring. Here the fact that, generally, a stable terminal state is achieved is utilized. While the problem of the stability of the terminal state and the beginning of bedload movement are primarily two different things, both processes are controlled by the turbulence in the proximity to the boundary, which in turn is determined by the controlling roughness element (the largest grains. Because both processes are clearly related to one another

it is permissible to conclude one thing from the other.

Concerning the stable end state the following general remarks are made:

The fact that the bottom shear stress undergoes turbulent fluctuations leads to the fact that even for smaller and smaller grains, during a given time the critical shear stress will not be exceeded and therefore a given percentage of this fraction will always be found at rest. The observations in the model now have shown that these finer fractions also are even set down in the stable top layer (see photographs 1 and 5). This can only be explained by the fact that the average eroding shear stress on the grain is smaller than the average bottom shear stress, which is probably due to the smaller grains lying nearer to the theoretical bed (i.e. deeper) than the larger grains. In other words: for the top layer to be stable the grains must be arranged according to a specific geometry.

The presence of small grains in the top layer was also observed by Lane and Carlson (12) in irrigation canals that have been in use for more than 70 years. This led to both authors giving up entertaining their hope that for a given average bottom shear stress, a critical grain size, so to speak, exists, which is a boundary between those grains of the mixture which are eroded, and which remain still, an assumption that Egiazaroff (3) made in an even more recent publication in order to investigate, at least as a first approximation, the problem of the partial bedload transport.

2.2 The Armoring Experiments

2.2.1 The experimental apparatus

The natural armoring of channel bottoms was investigated in a model which essentially consisted of the following parts (figure 4): inlet water pipe with a measuring device and valve for measuring and controlling the amount of water, channel inlet, channel measuring section, settling basin for the eroded material, sluice gate to regulate the flow condition in the channel, return pipe to the pump. During the experiments practically no sediment particles went into suspension (perhaps with the exception of part of the fine fraction which therefore was not considered in the evaluation of the experiments). Therefore it was not necessary to use a sediment recirculating system, returning the suspended sediments to the channel inlet.

A few especially important points concerning the experimental arrangement are pointed out below.

Channel length

An important provision for conducting the experiment is the existence of a constant average shear stress over the entire length of channel. This shear stress should not decrease during the experiment, otherwise it is not clear which shear stress controls the armoring process. However, in the literature it is often assumed that during an experiment, as the armoring experiments described in section 2.1, sediment transport only vanishes when a decrease in bed slope has decreased the bottom shear stress. But for channel bottoms which consist of mixtures, this decrease does not necessarily occur. At any place along the channel the same amount of degradation is required to accumulate enough course grains to prevent further erosion.

As a result the channel profile must remain parallel to the initial bed profile. In order to be able to prove this conclusively one must have a sufficiently long length of channel. Therefore at least some of the the experiments were carried out in a channel of approximately 40 meters in usable length.

- Channel width

For the calculation of the bottom shear stress the influence of the walls is to be considered; it is advantageous to hold the depth of flow small in proportion to the channel width. Thus, possible errors due to inadequacies in computing the influence of the wall will remain small. The channel width of 1 meter was always more than about five times the depth of flow. Consequently the necessary correction of the bottom shear stress because of the wall friction never amounted to more than about 15%. The method used for evaluating the influence of the wall is referred to in section 2. 3.

28

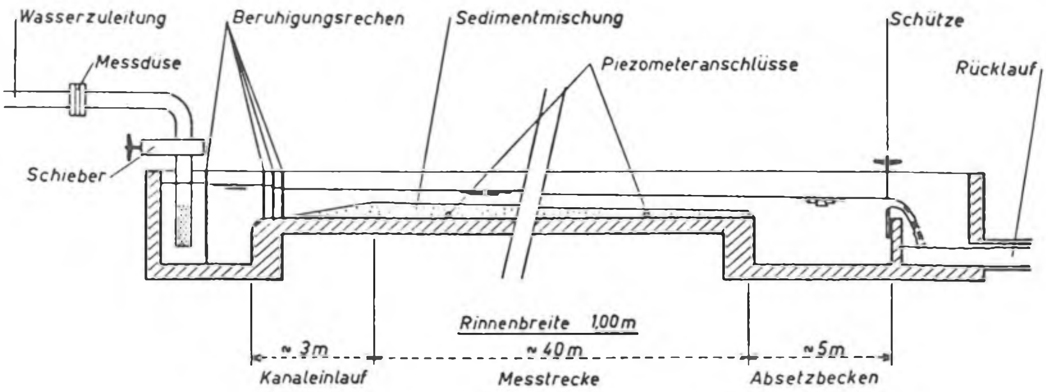

Figure 4. The experimental apparatus

- Bed slope

Because the condition of the ratio of the water depth to channel width had to be observed and only a limited channel height for the process was available, the possible variation of slope was limited. Experiments conducted in the 40 meter long channel were carried out with a 0.2 and 0.3% bottom slope. In order to have a broader experimental basis, experiments in a channel with a usable length of 5 meters and 40 cm wide were conducted with bed slopes of 0.2, 0.3 and 0.4%.

- Starting mixture

For a starting mixture two different sediment mixtures were used. The characteristic grain sizes are summarized in table 2*. The grain size distribution of the mixtures appears as it is commonly found in Swiss rivers. Essentially the grain sizes of the second mixture are twice as large as the first, serving first of all to expand the range of Reynolds numbers of the experiments. The fact that both grain size distribution curves (with $\frac{k}{k_{max}}$ as the abscissa, see fig. 5) depart from each other is unimportant because equation (8) which will be checked experimentally is not dependent on the starting grain size distribution.

---

* k_{90} is the grain diameter of which 90 percent of the weight of the grains are smaller. k_m is defined as

$$k_m = \sum_{i=1}^{n} k_i \, \Delta p_i$$

where Δp_i is the relative weight (as a fraction of one) of the n fraction with an average grain diameter k_i.

	Mixture 1	Mixture II
k_{max}	6.0 mm	12.0 mm
k_{90}	3.8 mm	9.1 mm
k_m	1.6 mm	3.1 mm

Table 2

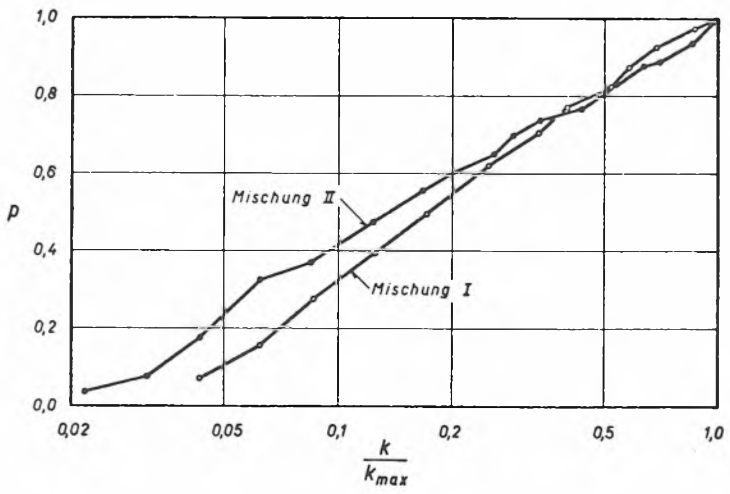

Figure 5. Grain size distribution curves for the gravel-sand-mixtures used.

- Measurement methods

a. Water discharge

An orifice was built into the entrance pipe to determine the water discharge in the long channel; it gave a measurement error under 2%. In the short channel a weir with the same accuracy was used.

b. Slope

In order to determine the piesometric water slope, perforated tubes were layed in the gravel-sand-mixture at five cross sections in the channel, and were connected to corresponding manometers. A hooked point gage was used to read each manometer. The average water surface elevation in the measurement cross section could be determined exactly to within one tenth of a millimeter. The bed slope was determined with the aid of a surveyor's level, by measuring [30] five points in each cross section every 4 meters. In order to be able to deduce the actual slope from the average heights at single measurement cross sections, an average straight line was passed through the measured points by the least squares method and the slope was determined from the slope of the line. In the short channel, water surface and bed elevations were determined with the aid of a movable point gage.

c. Depth of flow

The average depth of flow is given as the difference between the average water surface and bed elevations.

d. Grain-size distribution curve

By sieving a 2.0 kg sample by the standard method in sieves with square sieve openings the weight of each grain-size fraction was determined. The sieving took place in a shaking machine with four sieves placed one on top of each other, and shaken for 3 minutes. The grain-size distribution curves of the starting mixture and each of the eroded and top layer mixtures were determined. No difficulties were encountered taking a sample of the starting and eroded mixtures; taking a representative sample of the top layer requires a detailed explanation. As mentioned above the top layer is that upper layer of grains on the bed which protects the underlying material from further erosion. Due to its condition of formation it is merely "one grain thick". Therefore when one removes one grain from the top layer one finds beneath a material equal to that which originally formed the bed. This was confirmed to be true in all experiments (see photographs 2 and 7) and was also observed in nature by Lane and Carlson (12). It was therefore a question of developing a method that permitted obtaining exactly this layer of grains. After different preliminary experiments the following method was developed: after the conclusion of an experiment a border was placed around a section of top layer 20 x 20 cm. Into this border, liquid resin with a temperature of about 200°C was poured until all stones were covered completely (photograph 6). After a few minutes the border could be removed and furthermore a solid plate of resin was lifted out. Only the upper layer of grains adhered to the plate (photographs 7 and 8). Material that laid beneath the top layer, and due to its moisture developed some cohesion to the top layer, could easily be removed as soon as it was dry. In order to obtain a representative sample in this way 0.16 m^2 in the experiments with the first starting mixture, and 0.40 m^2 in the experiments with the second starting mixture were required. The resin was dissolved with an organic solvent and the cleaned grains were sieved according to the method mentioned above.

2.2.2. Typical experimental procedure

The carefully mixed starting mixture was put into the channel, during which time special attention was paid so as not to cause sorting of the mixture. The material was compacted as tight as possible by rodding under water. In order to flatten the bed and to give it the correct slope, laths of the proper height were placed every two meters in such a way that over the entire channel length an abundance of excess material existed. The surplus material was then removed from lath to lath. By removing enough excess material extensive sorting of the surface material was avoided (photograph 2*).

Then the laths were removed and the corresponding places patched. Immediately before an experiment the starting slope was once more measured with a surveyor's level.

The filling of the experimental channel with water was done very slowly in order to provide infiltration into the bed and displacement of as much air as possible. This was especially important in the region of the perforated tubes, which led to the manometers, in order to avoid possible errors due to air inclusion. Therefore, before a channel was entirely filled with water, water was put into the bed through the piezometer tubes; therefore, the air in the bed in the region of the perforated tubes was forced to the surface.

After the entire bed was under water, the discharge was increased from zero to the end value in a relatively short time. "Short" here means short in relation to the total duration of the

---

* Photographs 2 to 8 show the same bed surface area in the process of an experiment.

experiment; the increase in discharge always took place in between one-half and one and one-half hours. From the start, attention was paid to having normal flow conditions prevail in the channel, and therefore the depth of flow was constant over the entire channel. This could be accomplished by regulation of the sluice gate at the lower end of the settling tank. The discharge was held constant during the entire experiment. The gradual degradation of the bed due to progressive erosion made a corresponding lowering of the sluice gate necessary in order to keep normal flow conditions in the channel. The piezometers were used as the check on the water surface.

The development of the top layer in the process of the experiments could be clearly followed. In the first phase of the experiment selected material (the erosion mixture) was transported in the form of distinct ripples that reached a maximum height of between one and one and one-half times the maximum grain size of the starting mixture. These ripples formed simultaneously along the entire length of the channel at the beginning of an experiment. This phase was concluded after the most upstream ripple had reached the channel end.

During this process the formation of the top layer was 32
clearly observed. The larger stationary grains soon formed an identifiable layer that was only temporarily covered by the travelling ripples. As soon as the upstream end of the ripples had passed through the observation cross section, the same layer could again be recognized. (See photograph 3; in the upper half of the photograph the bed is being covered by a ripple; one already sees in the lower half; i.e. immediately downstream from the front of the ripple, the clearly formed top layer.)

During the second phase of the experiment the sediment transport had already strongly died away, in that no more ripples were formed. Rather strongly expressed secondary currents in the channel always drove the existing movable material together into separate parallel longitudinal stripes (photograph 4). Depending on the boundary conditions these stripes could be observed simultaneously over the entire channel length, or be only a few meters long. The number of secondary current stripes distributed across the channel width depended on the water depth, and were set up as if the secondary "rolling currents" in the cross section were square. With progressively larger time in the experiment the erodable material became scarce, and the secondary current stripes gradually disappeared, and at the end of the experiment an absolutely uniform type layer, according to the grain size distribution and thickness, resulted over the entire cross section and along the entire channel length (photograph 5).

In combination with the gradual building up of the top layer was an increase in the roughness for the flow condition. This caused a slight increase in the depth of flow and also in the bottom shear stress during the first part of the experiment. It was observed however, that this increase was ended as soon as the last ripple had reached the end of the channel, i.e. in other words, in the long channel this slight increase was over in a few hours, while the total duration of the experiment was in the order of between 150 and 250 hours. Therefore, without making further assumptions, the final water depth was controlling for the armoring process.

In general the experiment was brought to a close when the sediment transport per unit time fell below one-half of a percent of the sediment transport at the start of the experiment. As a control, the bed material collected in the settling tank was gathered and weighed. In this way it was possible to obtain the particle size distribution of the eroded material as a function of time (figure 6). After the end of the experiment the total of the mixture eroded by the water was 33 weighed under water and the grain size distribution curve of this mixture obtained. After the final bed slope was determined the top layer was removed by the method described above, (photographs 6 and 7) and its weight per unit surface area as well as its grain size distribution curve was measured.

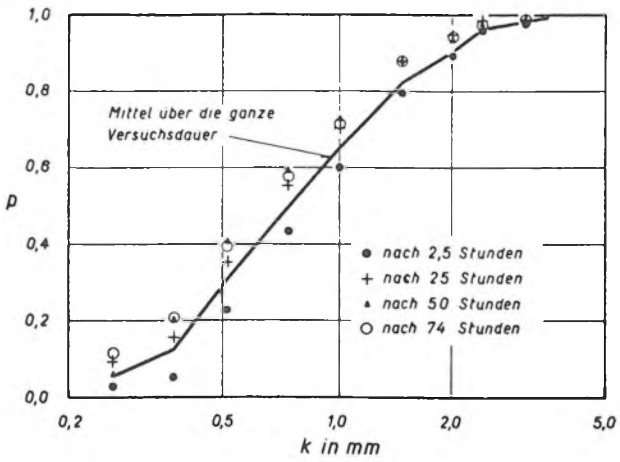

Figure 6. Grain size distribution curve of the eroded mixture as a function of time (Experiment No. 1/5).

2.3. Analysis of the Experimental Results

The following measured values were available for the analysis of the experiment: the final water depth h, the starting and final slope J, as well as the water discharge, also the size distribution curves of the starting, the eroded, and the top layer mixtures as well as the weight per unit surface area of the eroded and top layer mixtures. The first three hydraulic parameters served to determine the bottom shear stress, while the data pertaining to the grains, i.e. the grain size distribution curves and the weights per unit surface area, were used for the calculation of the probability of a single grain to remain at rest. Therefore the necessary data is available to be able to test equation (8), given in the first chapter.

2.3.1. Calculation of the bottom shear stress 34

During the experiment the original slope remained constant within the measuring accuracy of about 2%; in other words the bed was degraded parallel to its original line. Therefore, the requirement of a constant shear stress was fulfilled, and a proof provided for the condition that with flow in a channel with a bed made of a gravel-sand-mixture, the bedload transport can cease without causing a reduction in slope.

The average bottom shear stress for an infinitely wide channel is

$$\overline{\tau} = \gamma_w \, h \, J$$

$\bar{\tau}$ average bottom shear stress

γ_w specific weight of the fluid

h depth of flow

J energy slope

For the case of a channel of finite width the bottom shear stress is reduced due to the influence of the walls. It then is

$$\bar{\tau} = \gamma_w r_s J \tag{13}$$

where r_s is the hydraulic radius associated with the bed.

In the following it is shown that from the measured parameters h and J as well as the water discharge Q and channel width b the hydraulic radius associated with the bed can be calculated in order to determine the bed shear stress by equation (13).

Essentially the same assumptions are made here that were proposed by Einstein (5). The cross section is composed of separate parts, each with an area f_i, hydraulic radius r_i and roughness coefficient λ_i. The basis of the idea of Einstein was that all the individual cross section parts have the same energy slope, J, and the same average velocity $\bar{u}_m$*, and that the flow formula can be applied to each of the individual sub sections. However, while Einstein used the Manning flow formula, here the theoretically better established equation of Darcy-Weisbach is used.

$$J = \frac{\lambda}{4r} \cdot \frac{\bar{u}_m{}^2}{2g} \tag{14}$$

---

*The validity of this assumption will not be investigated here. Its applicability is proved sufficiently by the number of successes that were achieved with its use.

λ roughness coefficient

r hydraulic radius $r = \frac{f}{p}$

p wetted perimeter

f cross sectional area

$\bar{u}_m$ average velocity in the cross section f

(The index m with a parameter refers to the total cross section, i refers to a cross-section part.)

One uses equation (14) for only a single subsection part to give

$$\frac{\bar{u}_m^2}{8 g J} = \frac{r_1}{\lambda_1} = \frac{r_2}{\lambda_2} = \ldots\ldots = \frac{r_m}{\lambda_m} \qquad (15)$$

The total cross section f is the sum of the n cross-section parts

$$f = \sum_{i=1}^{n} f_i = \sum_{i=1}^{n} r_i\, p_i = \frac{\bar{u}_m^2}{8 g J} \sum_{i=1}^{n} \lambda_i\, p_i \qquad (16)$$

One places the expression from equation (15), $\frac{r_m}{\lambda_m}$, in front of the summation sign in equation (16) and replaces f by the product $r_m \cdot p_m$ giving the average roughness coefficient for the entire channel as the average of the friction values for the cross-section parts; the corresponding sum is

$$\lambda_m = \frac{1}{p_m} \sum_{i=1}^{n} p_i\, \lambda_i \qquad (17)$$

In order to be able to calculate the bottom shear stress one needs the hydraulic radius corresponding to the bed that is calculated according to equation (15)

$$r_s = \frac{\overline{u}_m^{\,2}}{8\,g\,J}\,\lambda_s \tag{18}$$

λ_s coefficient of roughness for the bed.

One calculates the roughness coefficient of the bed, λ_s, from equation (17). Considering that the experiments were carried out in a channel with a rectangular cross section, one obtains

$$\lambda_s = \lambda_m + \frac{2h}{b}\,(\lambda_m - \lambda_w) \tag{19}$$

b channel width 36

λ_w roughness coefficient of the wall

According to equation (15) the corresponding roughness coefficient, λ_m, for the entire cross section comes from measured values

$$\lambda_m = \frac{8\;g\;J}{\overline{u}_m^{\,2}} \cdot \frac{b \cdot h}{b + 2h} \tag{20}$$

The roughness coefficient for the wall, λ_w, follows from the assumption that the channel wall is hydraulically smooth. (See e.g. Schlichting (18).)

$$\frac{1}{\sqrt{\lambda_w}} = 2.0 \log \frac{4\,\overline{u}_m\,r_w}{\nu} \cdot \frac{\sqrt{\lambda_w}}{2.5} \tag{21}$$

r_w the hydraulic radius with respect to the wall.

For $Re_w = \frac{4\,\overline{u}_m\,r_w}{\nu} < 100{,}000$ the approximation by Blasius is used for equation (21), which contains λ explicitly

$$\lambda_w = \frac{0.316}{Re_w^{\;1/4}} \tag{22}$$

One inserts the expression for r_w given by equation (15) into the wall Reynolds number, R_w, in equation (22) and solves it for λ_w, consequently

$$\lambda_w = 0.302 \left[\frac{\nu}{\bar{u}_m} \cdot \frac{8 g J}{\bar{u}_m^2} \right]^{1/5} \tag{23}$$

Therefore, λ_w is a function of purely measurable parameters.

The roughness coefficient of the bed λ_s follows from λ_m, λ_w and equation (19). With these values the hydraulic radius with respect to the bed can be calculated with equation (18), and from it the bottom shear stress $\bar{\tau}$ can be calculated with equation (13).

2.3.2. Calculation of the probability of remaining stationary 37

Generally there are four different methods available to calculate the probability of remaining stationary.

(1) Calculation of the probability of remaining stationary on the basis of the grain size distribution curves of the top layer and erosion mixtures as well as their weights per unit surface area.

One adds the top layer and erosion mixtures according to their proportional weights so that the sum of both these mixtures make up the total of the grains that came in direct contact with the current for considering the question of "remaining stationary" or "not remaining stationary". Formulated for a single grain fraction this addition is

$$g_D \, \Delta p_{Di} + g_E \, \Delta p_{Ei} = (g_D + g_E) \, \Delta p_{Ai} \tag{24}$$

g_D weight per unit surface area of the top layer mixture

g_E weight per unit surface area of the erosion mixture

Δp_{Di} relative weight of the part of the grain fraction i in the top layer mixture

Δp_{Ei} relative weight of the part of the grain fraction i in the erosion mixture

Δp_{Ai} relative weight of the part of the grain fraction i in the starting mixture

(Δp is always a fraction of 1).

In equation (24) it is assumed that the sum of the top layer and erosion mixtures, must give the starting mixture. The correctness of this assumption is obvious, as long as the eroded layer is relatively thick as compared to the maximum grain diameter. However, if the eroded layer is on the average only a fraction of the maximum grain diameter thick, sorting of the surface layer during installation may have an influence on the results and the sum of the top layer and erosion mixture does not give exactly the starting mixture put in at the beginning of the experiment. Therefore, equation (24) is the definition equation for Δp_{Ai} , or generally for the starting mixture.

The probability for remaining stationary is given for the grain fraction i with the average grain diameter k_i as the ratio between the number of grains that remained stationary and the total number of grains that come in contact with the current.

$$q_i = \frac{g_D}{(g_D + g_E)} \cdot \frac{\Delta p_{Di}}{\Delta p_{Ai}} \qquad (25)$$

q_i probability of remaining stationary for the fraction i.

The chief advantage of this method of evaluation lies in the fact that possible sorting of the surface of the initial bed has no influence on the probability of remaining stationary.

(2) Calculation of the probability of remaining stationary on the basis of the grain size distribution curves of the top layer and starting mixtures

From the definition for q_i follows

$$\Delta p_{Ai} \cdot q_i = C_1 \cdot \Delta p_{Di} \qquad (26)$$

C_1 constant of proportionality

One sums the right and left hand sides in equation (26) for all n fractions, recalling that by definition $\sum_{j=1}^{n} \Delta p_j = 1$, there follows for C_1

$$\sum_{j=1}^{n} \Delta p_{Aj} \, q_j = C_1 \sum_{j=1}^{n} \Delta p_{Dj} = C_1 \qquad (27)$$

When one inserts the value for C_1 into equation (26) one obtains

$$q_i = \frac{\Delta p_{Di}}{\Delta p_{Ai}} \sum_{j=1}^{n} \Delta p_{Aj} \, q_j \qquad (28)$$

However, equation (28) does not give q_i explicitly. One recalls, however, that for $k \rightarrow \infty$ the probability of remaining stationary must be 1, so one can write

$$1 = \lim_{k \rightarrow \infty} \frac{\Delta p_D}{\Delta p_A} \cdot \sum_{j=1}^{n} \Delta p_{Aj} \, q_j \qquad (29)$$

And the probability of remaining stationary is found by

$$q_i = \frac{\Delta p_{Di}}{\Delta p_{Ai}} \lim_{k \to \infty} \frac{\Delta p_A}{\Delta p_D} \qquad (30)$$

The analysis of the experiment by equation (25) has shown that it is permissible to replace the limit of the ratio by $\frac{\Delta p_{Aj}}{\Delta p_{Dj}}$ when for that grain fraction the dimensionless grain diameter

$$K_j = \frac{(\gamma_s - \gamma_w)\, k_j}{\overline{\tau}} > 50 \qquad (31)$$

As a result of this simplification the error in q is less than 1%. 39

In order to be able to analyze the experiment according to equation (30), at least the largest grain size considered must fulfill the condition imposed by equation (31). Furthermore, the grain size distribution curves of the starting and top layer mixtures must be known. The advantage of this second method is that one need not know the weights per unit surface area of the top layer and erosion mixture not the grain size distribution curve of the erosion mixture.

(3) Calculation of the probability of remaining stationary on the basis of the grain size distribution curves of the erosion and starting mixtures.

An analogy to equation (26) gives

$$\Delta p_{Ai}\,(1 - q_i) = C_2\, \Delta p_{Ei} \qquad (32)$$

Here C_2 is calculated as

$$C_2 = \sum_{j=1}^{n} \Delta p_{Aj} \, (1 - q_j) \tag{33}$$

The probability of remaining stationary is then given by equations (32) and (33) as

$$q_i = 1 - \frac{\Delta p_{Ei}}{\Delta p_{Ai}} \sum_{j=1}^{n} \Delta p_{Aj} \, (1 - q_j) \tag{34}$$

Here again the sum can be evaluated by taking the limit of equation (34). The probability of eroding, e.g. 1 - q, increases as $k \to 0$. But as long as the bottom shear stress fluctuations are distributed according to the Gaussian normal distribution, the value of 1 - q will never reach 1 for k = 0. For a standard deviation of 0.57 (as was later found to be the case) the theoretical limiting value amounted to only 0.96.

$$0.96 = \lim_{k \to 0} \frac{\Delta p_E}{\Delta p_A} \sum_{j=1}^{n} \Delta p_{Aj} \, (1 - q_j) \tag{35}$$

The probability of remaining stationary is now calculated to be

$$q_i = 1 - 0.96 \, \frac{\Delta p_{Ei}}{\Delta p_{Ai}} \lim_{k \to 0} \frac{\Delta p_A}{\Delta p_E} \tag{36}$$

However, the extrapolation to k = 0 conceals considerable uncertainties. Therefore, it is desirable to insert the average value of the ratio $\frac{\Delta p_{Aj}}{\Delta p_{Ej}}$ of the fraction j with a dimensionless grain diameter of about 40
$3 < K_j < 10$ in the ratio $\frac{\Delta p_A}{\Delta p_E}$ where k = 0. With the foregoing assumption

for the distribution of the shear stress, the average value of the probability of being eroded equals about 0.92. Equation (36) can therefore be replaced by the equation

$$q_i = 1 - 0.92 \frac{\Delta p_{Ei}}{\Delta p_{Ai}} \left[\frac{\Delta p_{Aj}}{\Delta p_{Ej}} \right]_{3 < k_j < 10} \tag{37}$$

The advantage that this method of analysis has (as does the previous method) is that the weights per unit surface area of the top layer and erosion mixtures need not be known. While the determination of the grain size distribution curves of the top layer mixture presents some practical difficulties, the necessary grain size distribution curve of the erosion mixture required here is obtainable without difficulty.

(4) Calculation of the probability of remaining stationary on the basis of the grain size distribution curves of the starting, erosion,and top layer mixtures

From equations (28) and (34) q_i is directly determined

$$q_i = \frac{\Delta p_{Di}}{\Delta p_{Ai}} \frac{(\Delta p_{Ai} - \Delta p_{Ei})}{(\Delta p_{Di} - \Delta p_{Ei})} \tag{38}$$

A comparison of equation (29) with equation (38) shows that the former is the accrued sum calculated by means of an upper limit, while here the sum is replaced by a quotient that is calculated from measurements which can be made separately for each fraction. Equation (38) is ideal for a simple analysis. However, in respect to the propagation of errors, this method is extremely unfavorable. The differences put in the numerator and denominator, in part (especially in the interesting range of intermediate grain sizes), are of the order of magnitude of the measurement accuracy. The quotient $(\Delta p_{Ai} - \Delta p_{Ei})/(\Delta p_{Di} - \Delta p_{Ei})$ exhibits extreme scattering, when actually it should remain constant fraction to fraction, hence an analysis by this fourth method is impossible.

Therefore, the first three methods described above are available for the analysis of the experiments. It is shown, however, that due to special peculiarities of some experiments, one was not entirely free in the choice of the method.

Analysis by method (1) 41

Because of the possibility of the condition of sorting of the surface mixture this method is always given preference whenever possible. All experiments in the short channel with starting mixture I as well as two experiments with this mixture in the long channel were analyzed according to this method. Dispite the fact that the weight per unit surface area of the top layer for the same starting mixture must be an unequivocal function of the bottom shear stress considerable scatter was observed. The scatter is due to difficulties with the method for removing the top layer, as were described above. The grain size distribution of the top layer mixture, however, was not affected by this difficulty. In order to keep the influence of the scattering as small as possible, the weight per unit surface area of the top layer was plotted as a function of the bottom shear stress and a curve of best fit was drawn through the points. In the analysis of the experiments according to equation (25), a weight per unit surface area for the top layer was assumed according to the best fit line in figure 7.

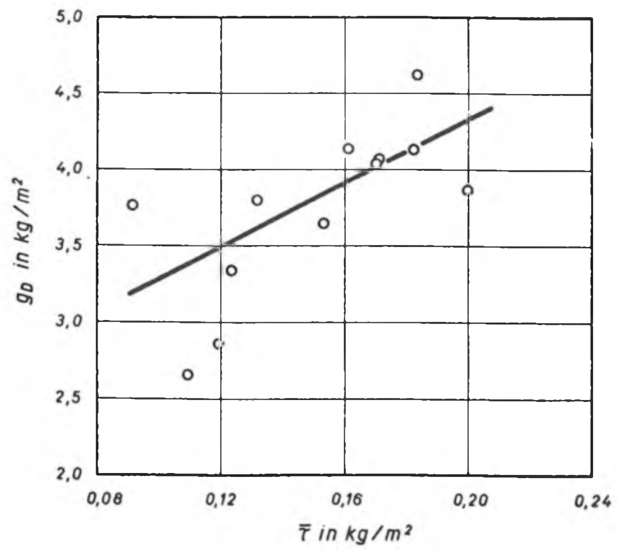

Figure 7. Weight of the top layer as a function of the average bottom shear stress (Starting Mixture I).

Analysis by method (2) 42

During the first phase of experiments in the long channel considerable ripple formation occurred. At high bottom shear stresses clearly it was possible that in this phase the larger components moved, but were only capable of being transported while they could roll unhindered on the smooth beds formed by the fine material. In principle these components would belong to the remaining stationary fraction. In the first phase of the experiments, therefore, under certain conditions a kind of slippage of material occurred, which probably was possible only because of the large bed deformations. Because the sum of the erosion and top layer mixtures must give the starting mixture, the slippage mixture must exhibit the same grain size distribution as the starting mixture. A careful analysis of the erosion mixture in these experiments in which this slippage occurred, showed that it is always factually possible to separate a certain amount from the erosion mixture, with a grain size distribution that agrees with the starting mixture. It would have been possible to analyze these experiments by method (1), using the "genuine" erosion mixture (total erosion mixture minus slippage) and top layer mixture. However, the separation of the slippage from the erosion mixture was hardly possible on objective grounds. Therefore, these experiments were analyzed according to method (2); i. e. according to equation (30).

Analysis by method (3)

During the experiments with starting mixture II an additional difficulty occurred in connection with the method of removing the top layer. The method of obtaining the top layer with the help of resin was developed especially for starting mixture I. The selection of the poured material was resin because it had most nearly met the requirement of exactly lifting out each top layer grain, about which actually the question "remaining stationary or not remaining stationary" was concerned. There probably were grains that locally came in contact with the current but were unremovable (in the process of pouring the resin), because they were partly covered by other grains. In general the contacting surfaces of these grains partially covered with resin was too small to stick while lifting out by resin plate. In the case of the second starting mixture it is seen that the grain diameter is approximately doubled, and consequently the contact surface between the grains and resin approximately quadruples. Partially covered grains, that strictly did not belong to the top layer, as a consequence of their essentially larger contact surface, showed a strong increased tendency

to stick to the resin during lifting out the top layer. This caused a systematic error in the grain size distribution as well as in the weight of the top layer. Therefore, in the analysis, the use of the grain size distribution curve as well as the weight per unit surface area of the top 43
layer must be abandoned. Because data pertaining to the erosion mixture were not affected by this phenomena, analysis by method (3) is considered. Now, to be sure, during the experiment attention must be paid to assure that no slippage occurs, or else the erosion mixture will also become contaminated. Also, the measurements in the Aare River above Lake Brienz were analyzed by method (3). They are referred to in section 3. 1.

In each experiment the probability of remaining stationary could now be determined as a function of the dimensionless grain diameter,

$$K = \frac{k(\gamma_s - \gamma_w)}{\bar{\tau}} .$$

A compilation of analyses of experiment No. 1/5 by methods (1), (2) and (3) is found. It is shown that method (1) gives the least scatter. But generally all three methods yield the same result (Fig. 11).

2. 3. 3. Determination of the critical shear stress

In section 1. 2 it is shown (equation (9)) that when the average bottom shear stress is equal to the critical shear stress of a specific grain the probability of remaining stationary is 0. 5. In each experiment by plotting the probability of remaining stationary as a function of the dimensionless grain diameter the dimensionless critical shear stress T_c could be picked off at the point q= 0. 5* (see figure 11).

---

* Because in the plotting of the function q = f(K) the measured points always exhibited a certain scattering, a curve of best fit was passed through the measured points. In the range where T_c is independent of Re_* this curve should be a straight line as long as the fluctuations of the bottom shear stress are normally distributed according to the Gaussian distribution, and it is drawn on probability paper. In the range $T_c = f(Re_*)$ a distortion takes place.

$$\tau_c = \left(\frac{1}{K}\right)_{q = 0.5} \tag{39}$$

The Reynolds number, $Re_* = \frac{u_* k}{\nu}$, for the grain size where $\tau_c = \bar{\tau}$ was calculated and the measured point was plotted in figure 8

The points measured by Shields are plotted in the same figure for those conditions that either a flat bed was obviously obtained, or with certainty the influence of the uneven bed could be eliminated.

Therefore, in reference to measurements in the laboratory made during this study direct observations of τ_c are available in a range of Reynolds numbers from about 55 to 230. With the measurements of Shields the range is extended down to a Reynolds number of 16. An extension going to higher Reynolds numbers results from the measurements in the Aare River. These measurements are at 44 the very high Reynolds number of about 10^4. Also, the value for τ_c at the highest Reynolds number already reached in the laboratory is in good agreement with that observed in the field, therefore it is likely that at the highest Reynolds number which occurred in the laboratory, τ_c is independent of Re_*. Egiazaroff (2) stated that this independence occurs at a Reynolds number of 200-300, while Iwagaki (8) stated a corresponding limiting value of about 170.

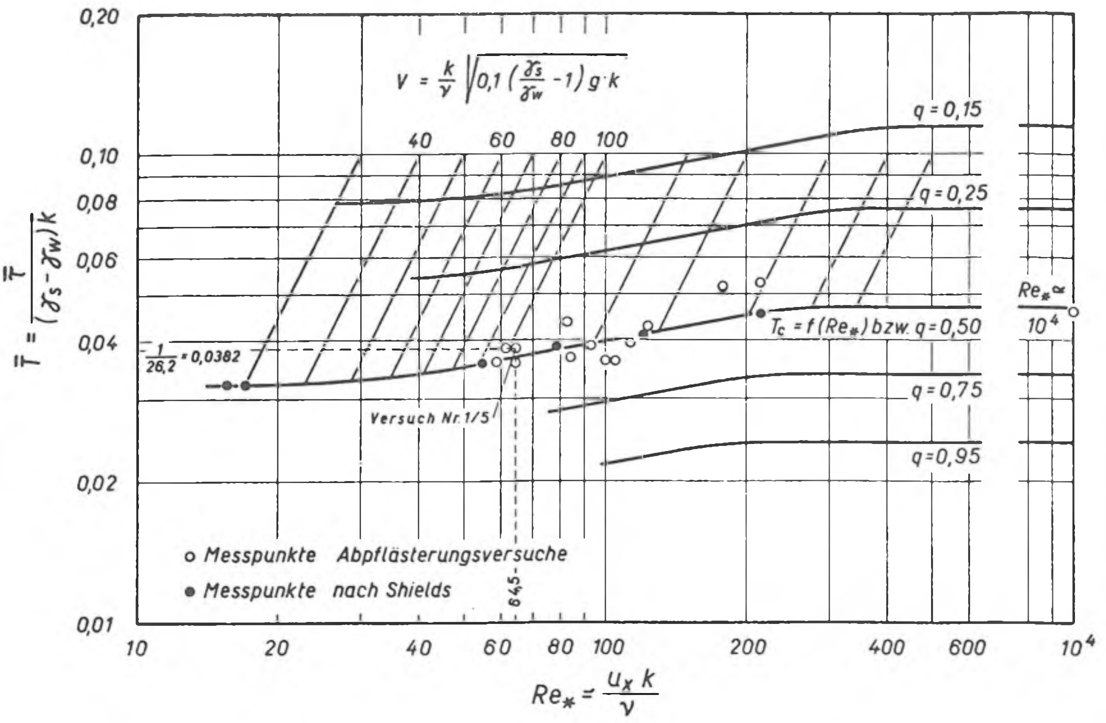

Figure 8. Dimensionless critical shear stress as a function of the Reynolds number of the grains. In the range of measurements made the curve for q = 0.5 is drawn (calculated on the basis of a standard deviation, σ = 0.57). The parameter V, suggested by Vanoni (18) facilitates the use of the figure.

The limiting value of T_c = 0.047 for Reynolds numbers greater than 200 was obtained by averaging the measured values for $Re_* > 200$. The value 0.047 is identical with that used by Meyer-Peter in his bed-load formula. He found this value by the same method as Shields, namely by extrapolation of the bedload function, and obtained an average value from numerous observations. (The requirement, that the bedload measurements had to be made at bottom shear stresses 45
that were relatively high in comparison to the critical, were considered fulfilled in the Meyer-Peter experiments. A correction was made for the influence due to the occurring of the bed forms.) Shields assumed

a limiting value of about 0.060 and believed that this value is reached only at very high Reynolds numbers. But actually his own measurements did not exceed about $Re_* = 200$. In the range $100 < Re_* < 200$ he observed an average T_c of about 0.045. Iwagaki gave a limiting value of 0.050. In general, limiting values for T_c quoted in the literature lie between 0.045 and 0.055; they are obtained theoretically (generally for spheres) or experimentally. As a result of neglecting the influence of secondary effects a certain scattering occurs.

The method exhibited here for the experimental determination of T_c is objective. However, T_c must be determined on the basis of a relatively complicated analysis of the measurements, which unfavorably influences the scatter. The average deviation of a single value from the curve of best fit amounted to about 7%.

Here it is especially emphasized once more that in the condition for movement

$$T = \frac{\tau}{(\gamma_s - \gamma_w)k} > T_c \qquad (6)$$

the instantaneous bottom shear stress is the controlling factor where T_c is a function of Re_* given in figure 8. Therefore, it is not true, as has often been supposed, that $\frac{\tau}{(\gamma_s - \gamma_w)k}$ must be at least 0.18, when depending on the trubulent intensity $\frac{\bar{\tau}}{(\gamma_s - \gamma_w)k}$ amounts to half or quarter of this value.

2.3.4. Determination of the statistical distribution of bottom shear stress.

Now after the function $T_c = f(Re_*)$ is known the critical shear stress can be calculated for each grain size in each experiment (i.e. for any average bottom shear stress). If q_i is that part of a grain fraction that remained as part of the top layer, then in q_i cases the critical shear stress of the fraction i was not exceeded. Or, one forms for each fraction the ratio $\tau_c / \bar{\tau}$ or T_c/T; then q_i states how often this ratio was not exceeded. For eroding the instantaneous bottom shear stress is controlling, one now forms

$$q = W\left(\frac{\tau}{\bar{\tau}} < \frac{\tau_c}{\bar{\tau}}\right) = f\left(\frac{\tau}{\bar{\tau}}\right) \tag{40}$$

the statistical distribution function of the instantaneous fluctuations of the bottom shear stress.

Each grain size fraction gives one point of this function per 46
experiment. The measured points are found in figure 9. The representation is on probability paper, on which a Gaussian normal distribution is portrayed by a straight line.

As always with bedload experiments a large scattering of the measured points occurred due to not considering secondary influences (as for example grain shape). A careful analysis shows that scattering is in part a systematic kind, and is due to the choice of the method of analysis. In general the points analyzed by method (3) lie higher than the average, while the points analyzed by method (2) generally lie too low. Those from the preferred method (1) lie in between.

One sees that considering the width of the scattering one can say that the distribution function determined in this indirect way can be approximated by a Gaussian normal distribution. The standard deviation was calculated as the minimal sum of the squares of the deviations of the measured points from the average Gaussian distribution. Simultaneously, the sum of the differences between the measured points and the average Gaussian distribution was approximately equal to zero.

The standard deviation was determined in this way as $\sigma = 0.57^{*}$. The average deviation at a single measured point from the average distribution curve amounts to about 0.09 (marked by the dotted line in figure 9). No single measured point lay more than three times the average deviation from the average value. Therefore these measurements verify that the statistical distribution of the fluctuations of the bottom shear stress can be considered as a Gaussian normal distribution for the treatment of the beginning of bedload movement of mixtures, as is done in equation (5) in section 1.2.

Einstein (7) called (as mentioned previously) σ a universal constant and used a value of $\sigma = 0.5$. The Gaussian distribution curves with $\sigma = 0.57$ and $\sigma = 0.5$ deviated from one another at most by an amount 0.03, compared with an average scattering of 0.09 for the measurements obtained here. The over one hundred measured points on the distribution function is good proof that the value of 0.57 found here might be correct. Generally, however, the difference can be called insignificant.

Here it is expressly pointed out that by checking equation 47
(8) with figure 9, it is independent of the grain size distribution of the starting mixture. The probability of remaining stationary for a certain size fraction therefore is not influenced by the percentage of
this fraction in the starting mixture. The amount of a fraction in 48

---

* The abscissa here is $\frac{\tau}{\bar{\tau}}$, σ is dimensionless (as in equation (8)), while in equations (5), (10) and (12) σ has the dimensions of a shear stress.

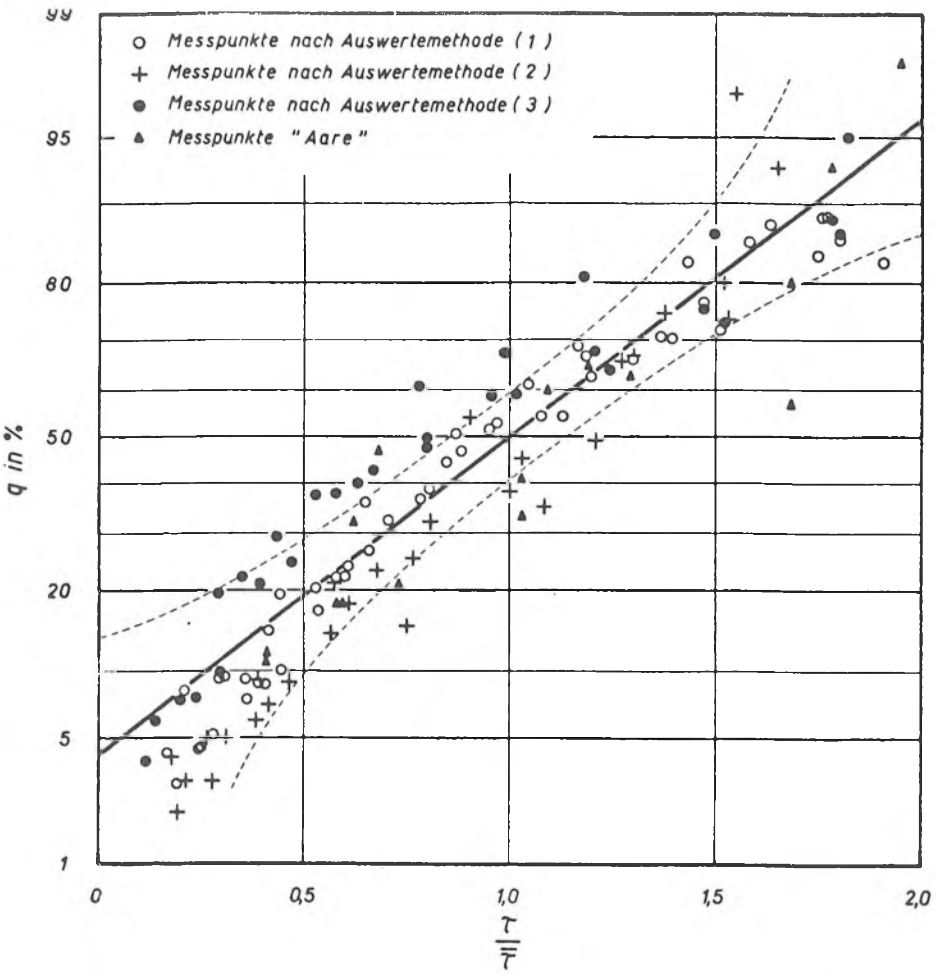

Figure 9. Statistical distribution of the fluctuation of the bottom shear stress

the top layer is proportional to the corresponding amount in the starting mixture, consequently, the grain size distribution of the top layer is dependent on the starting mixture.

In the appendix one finds a comparison between theory and experiment for experiment No. 1/5 in Table 6 and figure 12. One should observe that anamolies in the starting mixture are likewise copied in the theoretically calculated and measured grain size distribution curves of the top layer and erosion mixtures.

3. COMPARISON WITH FIELD MEASUREMENTS

3.1. The Aare River above Lake Brienz

From the fact that the grain size distribution curves of the material eroded from the channel practically do not change during the course of an experiment means that they are independent of how far the armoring process has progressed (see fig. 6); consequently, the grain size distribution curve of the erosion mixture is identical with the material that is transported in another channel with equal hydraulic conditions, in which bedload transport is in equilibrium. The bedload transport of a flow through an alluvium therefore corresponds, so to speak, to the transport in an armoring experiment in an infinitely long channel.

In order to be able to analyze the observations at a cross section in a manner equal to those from the armoring experiments described above, the particle size distribution curves of the alluvium as well as of the transported material, and the flow conditions must be known.

Generally, agreement can be expected in field observations only if some important presumptions are fulfilled: from a hydraulic standpoint the measuring section must meet some geometric specifications; correctly speaking, it must be a trapazoidal cross section with more or less a flat bed in order for the determination of the bottom shear stress to be clearly possible. Also a certain continuity in respect to the hydraulic and bed transport conditions must exist for a long reach of some length upstream from the measuring section, i.e. the stream should flow in a reach with relatively constant hydraulic conditions

through a homogeneous alluvium, and should have no important sediment or water inflows in this region. These requirements when applied
to a large scale problem are very stringent. Whether they are met in 49
a correct sense sufficiently, is shown to some degree by the results of the calculations.

Data used in the analysis contained herein was taken from the Office of Water Resources Report No. 33 for the Aare River above the Lake of Brienz for the year 1939 (4).

The above assumptions were fulfilled here to an exceptionally high degree. Above the measuring section "Wilerbrucke" at Brienzwiler was a reach about 8 km long without any significant inflow. The alluvium through which the Aare River flows is very homogeneous. The characteristic grain diameter k_{35} decreased uniformly through this reach as a result of abrasion from about 27mm to 24mm. One sees that the influence of abrasion is insignificant for the calculations; since all grain fractions are affected one can therefore say that the particle size distribution curve of the alluvium (the starting mixture) remains constant within a few percent throughout the entire length. The maximum grain diameter in the measuring section was about 270mm. The measuring section had a practically horizontal bed of about 14.80m in width. The sides had a slope of about 3:5. The energy slope on the average was 0.22%.

In the above report one finds data for depth of flow, energy slope, and grain size distribution curves of the transported material (therefore the erosion mixture) for the five discharges of 94, 115, 140, 180 and $215 m^3/s$, as well as the grain size distribution of the underlying material. The extremely uniform velocity distribution in the measuring section justifies the calculation of the bottom shear stress by the assumption of a logarithmic velocity distribution. From

$$\lambda_s = \left[2.21 + 2.03 \log \frac{r_s}{k_s}\right]^{-2}$$

(in which to the first approximation r_m can serve as r_s, and 270mm is inserted* for the maximum grain diameter k_s) follows

$$r_s = \lambda_s \frac{\overline{u}_m^2}{8 g J}$$

The quantity $\overline{u}$ is calculated from the data for discharge and water depth. From it the bottom shear stress $\overline{\tau} = \gamma_w r_s J$ is determined.

The calculation of the probability of remaining stationary was done by method (3) in a similar way as is shown in the Appendix for experiment No. 1/5.

The determination of T_c for each individual discharge was 50
abandoned. At the high Reynolds numbers Re_*, as occurred in the field, T_c is independent of Re_*, it is permissible to analyze the measured points $q_i = f(K_i)$ for different discharges collectively. A $T_c = 0.046$ results for $q = 0.5$. The points $q = f(\frac{\tau}{\overline{\tau}})$ are shown in figure 9.

Although one can expect that the uncontrolled secondary influences in nature strongly broaden the scatter it is seen that the value for T_c as well as the measured points in the diagram $q = f(\frac{\tau}{\overline{\tau}})$

---

* An analysis of laboratory experiments indicates that for the use of k_s, k_{max} is controlling.

lie in the range of the scatter field of the laboratory measurements. In regards to the same diagram, the average deviation of the single points during the field observations amounted to 0.12 compared with 0.09 during the laboratory observations. These results speak well of the way the assumptions were fulfilled.

3.2. Irrigation Canal in the San Luis Valley, Colorado

The above quoted authors Lane and Carlson (12) described remarkably clearly the phenomenon of armoring on the basis of observations in irrigation canals in the San Luis Valley, Colorado, U. S. A. They emphasized two points of special importance:

(1) the top layer is one grain thick

(2) in the top layer are found all grain sizes that are contained in the underlying starting mixture.

In this work Lane and Carlson gave the hydraulic data and the grain size distribution curves of the starting as well as the top layer mixture for a large number of canals. In respect to the hydraulic characteristics, the canal is ideal because in an irrigation canal the controlled maximum water discharge is known relatively well, and actually remains uniform for a long time. These characteristics are similar to the armoring experiments in the laboratory. In principle an analysis according to method (2) would be possible.

However for such an analysis the data pertaining to the particle size distribution curves was insufficient because the grain fractions were chosen too wide and because in the case of the top layer no numerical data for the fine material were given. The limits of the

size fractions stated by Lane and Carlson formed a geometric series with a factor of 2. As a result, the probabilities of remaining still for the individual fractions were far apart, especially in the entire range of the important larger components. Therefore, an accurate 51
analysis of the data is not possible.

When one calculates the grain size distribution curves of the top layer using the theory given above (the calculation for test reach 12 is carried out in the appendix), one sees from a comparison with the observed particle size distribution curve, that it is systematically too coarse, which is due to taking an incomplete top layer sample in the field.

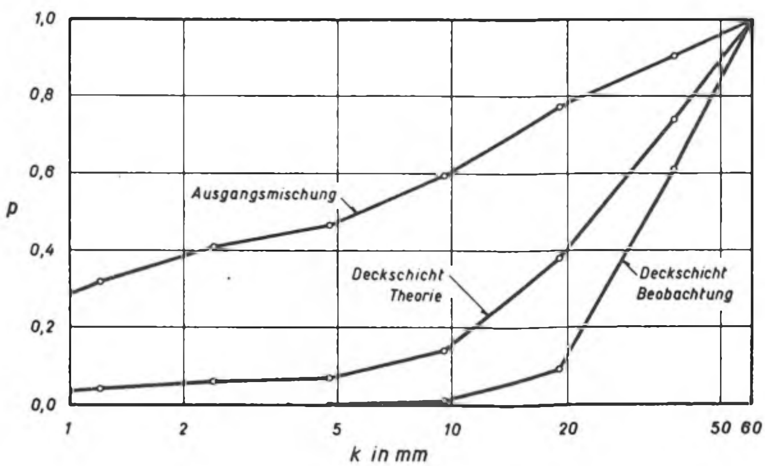

Figure 10. Particle size distribution curve of the top layer in test reach 12 in San Luis Valley, Colorado.

4. SUGGESTED POSSIBILITIES FOR ADDITIONAL INVESTIGATIONS

When writing in detail on the problems in this work questions arose which were not discussed further. Therefore some possible questions are pointed out.

4.1. Turbulence Measurements in the Proximity of a Rough Boundary

The assumption that the standard deviation, σ, of the fluctuations of the bottom shear stress is a constant is probably true in the range of Reynolds numbers investigated here. The scattering of the measured points does not cause one to say otherwise. It is always probable 52
that σ (as discussed above) in a certain range is a function of the Reynolds number of the grains (probably the Reynolds number of the maximum grain size $\frac{u_* k_{max}}{\nu}$. It is also assumed that this dependence ceases and σ is constant when the controlling Reynolds number exceeds a certain limit. This limiting value should correspond to the corresponding limiting value of the function $T_c = f(Re_*)$, i.e. it should lie at about $Re_* = 200$. Because only in a few experiments was the controlling Reynolds number significantly smaller than this value, the assumption, σ = constant, made here is justified.

For an exact investigation of σ, the indirect method of determination used here is unsuitable. In order to go further one must make direct turbulence measurements, in which one measures, in the proximity of a rough wall, the stagnation pressures which are proportional to the bottom shear stress and/or their fluctuations. Compensating for the influence of surface waves by the use of simultaneous measurements of the static pressures is not permissible, because these measurements are affected by cross currents and the dynamic and static measurements cannot be carried out sufficiently close to one another. In order to eliminate the errors due to surface waves one must make the measurements in a closed channel. Measurements made in such a manner will show under what conditions it is possible to express the statistical distribution of the fluctuations of stagnation pressures and/or bottom shear stress by a Gaussian normal distribution, and in what respect the standard deviation is dependent on the controlling Reynolds number.

Apart from these purely statistical interpretations of such measurements perhaps they also will give results on the effective structure of turbulence in the proximity of a rough boundary.

4.2. Investigations on the Necessary Amount of Erosion Required to Stabilize a Bed

With the help of equation (8) the probability of not eroding or eroding can be calculated. From equations (26) and (32) result the particle size distribution curves of the top layer and erosion mixtures. But the question of how much material must be eroded to form a stable bed has not been treated here. The reason it was not treated lies in the temporary existence of the above mentioned slippage, whose occurrence and amount depended on conditions that were not controlled here. If one assumes that this slippage is equal to zero, one can 53
make some statements.

From equations (25) and (26) results the ratio of the weights per unit surface area of the top layer and the sum of the top layer and erosion mixture.

$$\frac{g_D}{g_D + g_E} = \sum_{j=1}^{n} q_j \, \Delta p_{Aj} \tag{41}$$

If the top layer is only one grain thick the weight per unit surface of the top layer g_D can be estimated from the known grain size distribution. The fraction k_i of the top layer consists of s_i grains

$$s_i = \frac{6 \; \Delta p_{Di} \; g_D}{\pi \; A_v \, k_i^3 \; \gamma_s}$$

where A_v is a volume factor dependent on the grain shape, given by the ratio of the volume of the grains k_i to spheres with a diameter k_i. The surface covered by a single grain of the fraction k_i is

$$f_{ei} = \frac{\pi}{4} \, A_f \, k_i^2$$

where A_f is a surface factor dependent on the grain shape given by the ratio between cross sectional area of a grain of k_i to that of a sphere of diameter k_i. The entire fraction k_i requires an area of

$$\Delta f_i = s_i \cdot f_{ei} = \frac{3}{2} \cdot \frac{A_f}{A_v} \cdot \frac{\Delta p_{Di} \; g_D}{k_i \cdot \gamma_s}$$

when arranged in a layer one grain thick. Because all n fractions of the top layer collectively cover the total surface area one obtains $\sum_{j=i}^{n} \Delta f_j = 1$. From this follows the weight per unit surface area of the top layer

$$g_D = \frac{2}{3} \left[\frac{A_v}{A_f}\right] m \frac{\gamma_s}{\sum_{j=1}^{n} \frac{\Delta p_{Dj}}{k_j}} \qquad (42)$$

Because the factors A_v and A_f depend on the grain shape and generally vary with the grain size, an average value of the ratio $\frac{A_v}{A_f}$ must be chosen for equation (42). This ratio is a measure of the "flatness" of the grains. One approximates the grains by ellipsoids with semi axis of a, b, and c, where $a > b > c$, and because the grains usually lie so that the short axis is vertical one obtains

$$\frac{A_v}{A_f} = \frac{c}{b}$$

The weight per unit surface area results from equation (41) 54

$$g_E = g_D \left[\frac{1}{\sum_{j=1}^{n} q_j \, \Delta p_{Aj}} - 1\right] \qquad (43)$$

As already mentioned equation (43) with g_D from equation (42) can only give an estimate of the required minimum value. In order to be able to make an exact analysis of the weight per unit surface area of the erosion mixture additional investigations are required in which slippage must be particularly observed.

4.3. Investigations on the Identities of the Particle Size Distributions of the Moving Materials in Pure Armoring Experiments and in Experiments with Continuous Recirculation of the Bedloads

On the basis of fundamental considerations it is shown in section 3.1 that the particle size distribution curve of the erosion mixture is identical to the transported material under equilibrium transport rate conditions with equal hydraulic conditions. This was confirmed by the measurements in the Aare River above Lake Brienz. In spite of this, corresponding laboratory experiments are desirable. The experiments must be arranged the same way as were the pure armoring experiments. The erosion mixture of the material making up the channel must also be added to the flow in the channel (continuous recirculation of bedload transport). In this case as a result of the selection process a top layer is again formed, over which the sediment transport takes place. But special observations must be made of the possibility of when and under what circumstances slippage can occur. The analysis of the measurements from the Aare River apparently shows that no slippage had occurred.

APPENDIX

1. Analysis of Experiments 1/5

1.1. Determination of the average bottom shear stress

Given and/or measured values:

water discharge	$Q = 31.5$ l/sec
water depth	$h = 0.0699$ m
slope	$J = 0.00199$
channel width	$b = 1.00$ m
kinematic viscosity (at 15°C)	$\nu = 1.15 \times 10^{-6}\, m^2/sec$
acceleration due to gravity	$g = 9.81\, m/sec^2$
average velocity in the cross section	$\bar{u}_m = \frac{Q}{bh} = 0.451$ m/sec

The average roughness coefficient of the entire cross section is calculated by equation (20)

$$\lambda_m = \frac{8\,g\,J}{\bar{u}_m^2} \cdot \frac{bh}{b + 2h} = 0.0472$$

The roughness coefficient of the wall is calculated by equation (23)

$$\lambda_w = 0.302 \left[\frac{\nu}{\bar{u}_m} \cdot \frac{8\,g\,J}{\bar{u}_m^2}\right]^{1/5} = 0.0218$$

The roughness coefficient of the bed is calculated from λ_m and λ_w by equation (19)

$$\lambda_s = \lambda_m + \frac{2h}{b} (\lambda_m - \lambda_w) = 0.0508$$

The hydraulic radius with respect to the bed is calculated by equation (18)

$$r_s = \frac{\overline{u}_m^2}{8 g J} \lambda_s = 0.0661 \mathrm{m}$$

The average bottom shear stress results from equation (13)

$$\overline{\tau} = \gamma_w \, r_s \, J = 0.132 \ \mathrm{kg/m^2}$$

and the corresponding shear velocity is 56

$$u_* = \sqrt{\frac{\overline{\tau}}{\rho_w}} = 0.0359 \ \mathrm{m/s}$$

1.2. Determination of the probabilities of remaining stationary according to methods of analysis (1), (2) and (3)

Given and/or measured or calculated values:

average bottom shear stress	$\overline{\tau} = 0.132 \ \mathrm{kg/m^2}$
particle size distribution curves of the top layer, erosion and starting mixture	Δp_D, Δp_E, Δp_A
weight per unit surface area of the top layer	$g_D = 3.80 \ \mathrm{kg/m^2}$
weight per unit surface area of the erosion mixture	$g_E = 6.29 \ \mathrm{kg/m^2}$
specific weight of the grains	$\gamma_s = 2680 \ \mathrm{kg/m^3}$

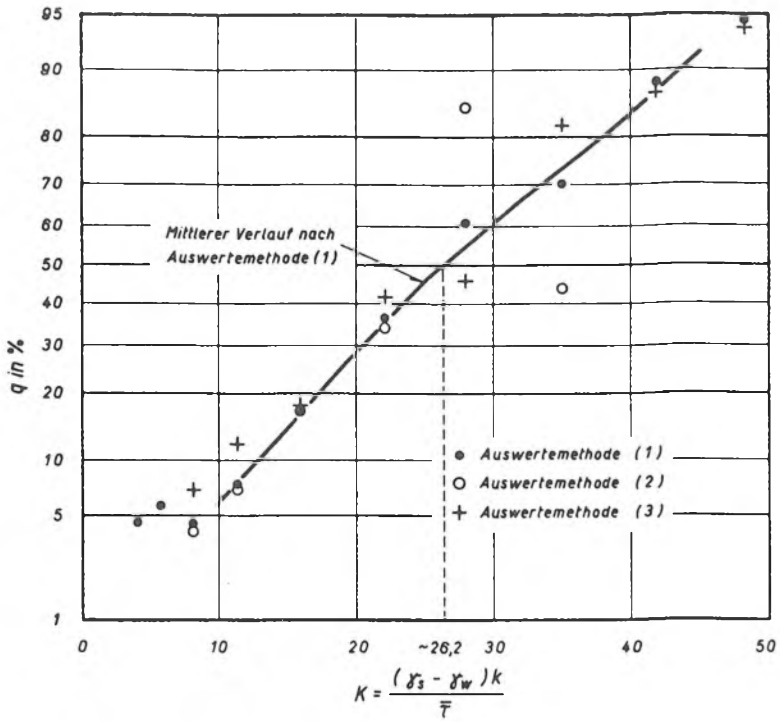

Figure 11. Probability of remaining stationary as a function of the dimensionless grain diameter computed according to methods of analysis (1), (2) and (3) for experiment No. 1/5.

In tables 3 to 5 are found the calculations of the probabilities 57
of remaining stationary by the three methods (see section2. 3. 2). The quantity q is plotted in figure 11 as a function of the dimensionless grain diameter $K = \frac{1}{\overline{T}}$. The critical bottom shear stress results from $T_c = \frac{1}{K}$ at the place q = 0. 5 or 50%. This value was plotted in figure 8.

From figure 8 results now the corresponding T_c for each grain size. The ratio $\frac{T_c}{\overline{T}}$ is found and listed in table 3. This is the ratio between the effective and average bottom shear stress $\frac{T}{\overline{T}}$, at which the corresponding grain comes into motion. The quantity q is plotted in figure 9 as a function of this ratio (i. e. the statistical distribution of the fluctuation of the bottom shear stress).

2. Comparison of Theory and Measurement

2.1. Experiment No. 1/5

The hydraulic data are assumed to be known (see Appendix section 1.1).

The dimensionless critical shear stress for each grain fraction is obtained from figure 8. On the basis of the ratios $\frac{T_c}{\overline{T}} = \frac{\tau}{\overline{\tau}}$ the probability of remaining stationary results from figure 9 with $\sigma = 0.57$.

Equation (28) yields

$$\Delta p_{Di} = \frac{q_i \Delta p_{Ai}}{\sum_{j=1}^{n} q_j \Delta p_{Aj}}$$

The particle size distribution curve of the top layer, $p_D = f(k)$, is given by a sum of Δp_{Di} over all fractions.

The particle size distribution curve of the erosion mixture is calculated similarly, where Δp_{Ei} results from equation (34)

$$\Delta p_{Ei} = \frac{(1-q_i)\ \Delta p_{Ai}}{\sum_{j=1}^{n} (1-q_j)\ \Delta p_{Ai}}$$

The calculations are carried out in table 6. The calculated as well as measured grain size distribution curves are drawn in figure 12. The fraction $k < 0.260$ mm was omitted from the comparison in the figure because in the experiment this fraction obviously went into partial suspension, therefore the expression for the calculated probability of remaining stationary for this function, in comparison to the one next to it, increases markedly. (This is caused by the partial absence of this grain size in the erosion mixture.)

2.2. The field observations in the San Luis Valley, Colorado

Given and/or measured or calculated values:

water discharge	$Q = 3.63\ m^3/sec$
depth of flow	$h = 0.54\ m$
slope	$J = 0.00243$
average velocity in the cross section	$\overline{u}_m = 1.22\ m/sec$
particle size distribution curve of the starting mixture	Δp_A
average bottom shear stress	$\overline{\tau} = 1.17\ kg/m^2$

The calculations of the particle size distribution curve of the top layer was done the same way as in the previous section (experiment No. 1/5) and are carried out in table 7. Theory and measurements are compared in figure 10. Comments on this figure are found in section 3.2.

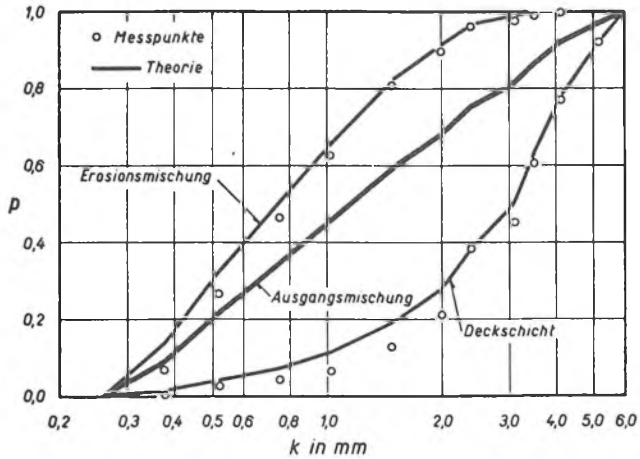

Figure 12. Comparison between theory and experiment for experiment No. 1/5.

k mm	k_I mm	Δp_D	$g_D \Delta p_D$ kg/m^2	Δp_E	$g_E \Delta p_E$ kg/m^2	$(g_D + g_E)\Delta p_A$ kg/m^2	q	K	$\bar{T}$	T_c	$\frac{T_c}{\bar{T}}$	Re_*
		0.011	0.042	0.000	0.000	0.042	1.000					
6.00												
	5.60	0.067	0.255	0.001	0.006	0.261	0.971	71.3	0.0140	0.0464	3.31	175
5.20												
	4.65	0.146	0.555	0.004	0.025	0.580	0.960	59.1	0.0169	0.0455	2.69	145
4.10												
	3.79	0.161	0.612	0.005	0.031	0.643	0.945	48.3	0.0207	0.0439	2.12	118
3.48												
	3.29	0.148	0.562	0.011	0.069	0.631	0.886	41.9	0.0239	0.0422	1.77	103
3.10												
	2.75	0.070	0.266	0.017	0.107	0.373	0.703	35.0	0.0286	0.0398	1.39	85.9
2.40												
	2.20	0.166	0.631	0.061	0.384	1.015	0.610	28.0	0.0357	0.0373	1.05	68.6
2.00												
	1.74	0.082	0.312	0.083	0.522	0.834	0.364	22.1	0.0452	0.0355	0.78	54.3
1.48												
	1.25	0.062	0.236	0.171	1.069	1.305	0.170	15.9	0.0629	0.0338	0.54	39.0
1.02												
	0.885	0.021	0.080	0.152	0.956	1.036	0.075	11.3	0.0885	0.0323	0.37	27.6
0.75												
	0.635	0.016	0.061	0.189	1.189	1.250	0.045	8.1	0.123	0.0310	0.25	19.8
0.52												
	0.448	0.020	0.076	0.186	1.170	1.246	0.057	5.7	0.175			
0.375												
	0.318	0.006	0.023	0.064	0.403	0.426	0.046	4.1	0.247			
0.260												
	0.130	0.025	0.095	0.056	0.352	0.447	0.202	1.7	0.606			

Table 3. Data from experiment No. 1/5 analyzed by method (1)

k mm	k_i mm	Δp_D	Δp_A	$\frac{\Delta p_D}{\Delta p_A}$	q	K
		0.011				
6.00						
	5.60	0.067	0.027	2.54	0.88	71.3
5.20						
	4.65	0.146	0.047	3.08	1.06	59.1
4.10						
	3.79	0.161	0.053	3.07	1.06	48.3
3.48						
	3.29	0.148	0.048	3.08	1.06	41.9
3.10						
	2.75	0.070	0.055	1.27	0.44	35.0
2.40						
	2.20	0.166	0.066	2.47	0.85	28.0
2.00						
	1.74	0.082	0.084	0.98	0.34	22.1
1.48						
	1.25	0.062	0.122	0.50	0.17	15.9
1.02						
	0.885	0.021	0.102	0.21	0.07	11.3
0.75						
	0.635	0.016	0.118	0.13	0.04	8.1
0.52						
	0.448	0.020	0.120	0.16	0.06	5.7
0.375						
	0.318	0.006	0.084	0.07	0.02	4.1
0.260						
	0.130	0.025	0.073	0.34	0.12	1.7

$$\left[\lim_{k \to \infty} \frac{\Delta p_A}{\Delta p_D}\right]^{-1} \equiv \frac{2{,}54 + 3{,}08 + 3{,}07}{3} = 2{,}90$$

Table 4. Data from experiment No. 1/5 analyzed by method (2)

k mm	k_i mm	Δp_E	Δp_A	$\frac{\Delta p_E}{\Delta p_A}$	1 - q	q	K
6.00	5.60	0.001	0.027	0.04	0.02	0.98	71.3
5.20	4.65	0.004	0.047	0.07	0.04	0.96	59.1
4.10	3.79	0.005	0.053	0.10	0.06	0.94	48.3
3.48	3.29	0.011	0.048	0.23	0.13	0.87	41.9
3.10	2.75	0.017	0.055	0.31	0.18	0.82	35.0
2.40	2.20	0.061	0.066	0.92	0.54	0.46	28.0
2.00	1.74	0.083	0.084	0.99	0.58	0.42	22.1
1.48	1.25	0.171	0.122	1.40	0.82	0.18	15.9
1.02	0.885	0.152	0.102	1.50	0.88	0.12	11.3
0.75	0.635	0.189	0.118	1.60	0.93	0.07	8.1
0.52	0.448	0.186	0.120	1.55	0.91	0.09	5.7
0.375	0.318	0.064	0.084	0.76	0.44	0.56	4.1
0.260	0.130	0.056	0.073	0.77	0.45	0.55	1.7

$$\left[\left(\frac{\Delta p_{Aj}}{\Delta p_{Ej}}\right)_{3<K_j<10}\right]^{-1} = \frac{1,60+1,55}{2} = 1,58$$

Table 5. Data from experiment No. 1/5 analyzed by method (3)

k mm	k_I mm	$\bar{T}$	T_c	$\frac{T_c}{\bar{T}}$	q	Δp_A	$q\Delta p_A$	Δp_D	p_D	$(1-q)\Delta p_A$	Δp_E	p_E
6.00									1.000			1.000
	5.60	0.0140	0.0464	3.31	1.00	0.027	0.027	0.079		0.000	0.000	
5.20									0.921			1.000
	4.65	0.0169	0.0455	2.69	1.00	0.047	0.047	0.137		0.000	0.000	
4.10									0.784			1.000
	3.79	0.0207	0.0439	2.12	0.97	0.053	0.051	0.149		0.002	0.003	
3.48									0.635			0.997
	3.29	0.0239	0.0422	1.77	0.91	0.048	0.044	0.127		0.004	0.006	
3.10									0.508			0.991
	2.75	0.0286	0.0398	1.39	0.75	0.055	0.041	0.120		0.014	0.021	
2.40									0.388			0.970
	2.20	0.0357	0.0373	1.05	0.53	0.066	0.035	0.102		0.031	0.047	
2.00									0.286			0.923
	1.74	0.0452	0.0355	0.78	0.35	0.084	0.029	0.086		0.055	0.084	
1.48									0.200			0.839
	1.25	0.0629	0.0338	0.54	0.21	0.122	0.026	0.075		0.096	0.147	
1.02									0.125			0.692
	0.885	0.0885	0.0323	0.37	0.135	0.102	0.014	0.040		0.088	0.134	
0.75									0.085			0.558
	0.635	0.123	0.0310	0.25	0.095	0.118	0.011	0.033		0.107	0.163	
0.52									0.052			0.395
	0.448	0.175	0.0310	0.18	0.075	0.120	0.009	0.026		0.111	0.169	
0.375									0.026			0.226
	0.318	0.247	0.0310	0.13	0.065	0.084	0.005	0.016		0.079	0.121	
0.260									0.010			0.105
	0.130	0.606	0.0310	0.05	0.048	0.073	0.004	0.010		0.069	0.105	
						$\Sigma q\Delta p_A = 0.343$		$\Sigma(1-q)\Delta p_A = 0.656$				

Table 6. Calculation of the particle size distribution of the erosion mixtures for experiment No. 1/5 with the help of the theory developed herein

k mm	k_i mm	$\bar{\tau}$	τ_c	$\frac{\tau_c}{\bar{\tau}}$	q	Δp_A	$q\Delta p_A$	Δp_D	p_D
60.0									1.00
	49.0	0.0142	0.047	3.31	1.00	0.092	0.092	0.26	
38.1									0.74
	28.6	0.0242	0.047	1.94	0.95	0.132	0.125	0.36	
19.05									0.38
	14.3	0.0485	0.047	0.97	0.48	0.179	0.086	0.24	
9.53									0.14
	7.15	0.0970	0.047	0.48	0.18	0.133	0.024	0.07	
4.76									0.07
	3.57	0.196	0.043	0.22	0.09	0.054	0.005	0.01	
2.38									0.06
	1.79	0.388	0.036	0.09	0.06	0.092	0.006	0.02	
1.19									0.04
	0.89	0.779	0.032	0.04	0.05	0.120	0.006	0.02	
0.59									0.02
	0.44	1.58	0.032	0.02	0.04	0.101	0.004	0.01	
0.30									0.01
	0.15	4.62	0.032	0.01	0.04	0.097	0.004	0.01	
						$\Sigma q\Delta p_A$	= 0.352		

Table 7. Calculation of the particle size distribution of the top layer mixture for test-section 12 in the San Luis Valley, Colorado

Versuchs-Nr.	Ausgangs-mischung	k_{max} mm	Q m^3/s	h m	b m	J ‰	$\bar{\tau}$ kg/m^2
1/ 2	I	6.0	0.0358	0.0720	1.00	2.50	0.171
1/ 5	I	6.0	0.0315	0.0699	1.00	2.00	0.132
1/ 6	I	6.0	0.0400	0.0814	1.00	2.00	0.153
1/ 7	I	6.0	0.0465	0.0911	1.00	2.00	0.170
1/ 8	I	6.0	0.0523	0.0979	1.00	2.00	0.182
1/ 9	I	6.0	0.0126	0.0710	0.40	2.00	0.123
1/10	I	6.0	0.010	0.0620	0.40	2.00	0.109
1/12	I	6.0	0.0118	0.0603	0.40	3.00	0.161
1/13	I	6.0	0.0109	0.0550	0.40	4.00	0.200
1/15	I	6.0	0.0516	0.0970	1.00	2.03	0.183
1/16	I	6.0	0.0269	0.0642	1.00	1.95	0.119
2/18	II	12.0	0.0649	0.1057	1.00	3.00	0.298
2/19	II	12.0	0.0867	0.1279	1.00	2.97	0.353
Aare		270	94-215	2.2-3.5	15.0	2.0-2.4	4.6-5.7

Table 8. Summary of experimental data

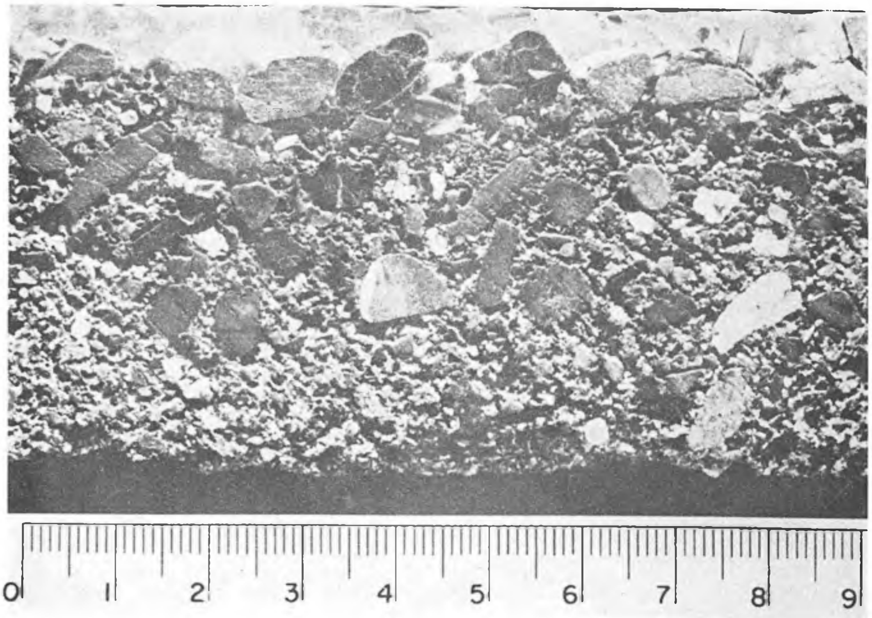

Photograph 1: Armored bed in cross-section, starting mixture II; the section was obtained with the help of resin

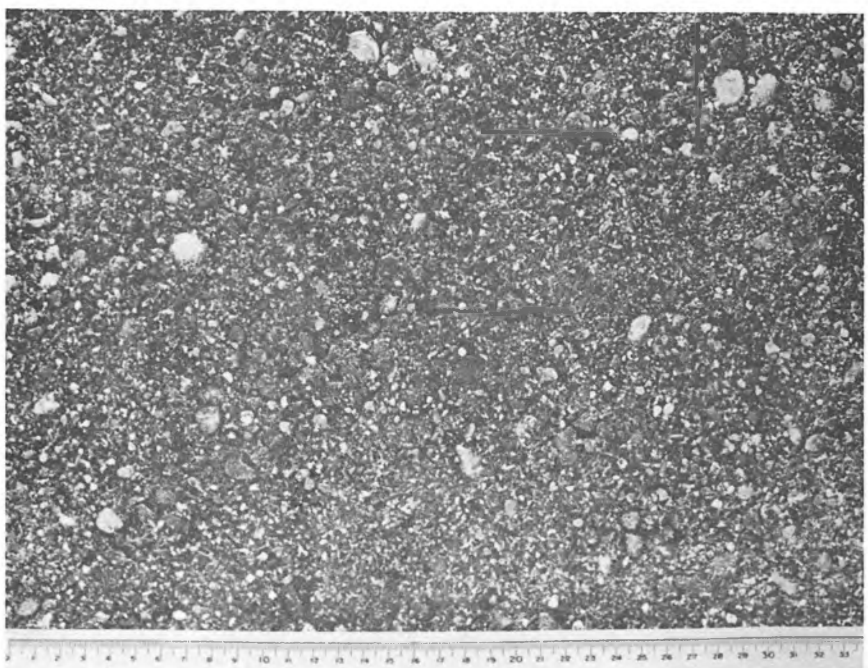

Photograph 2: bed surface before start of experiment starting Mixture II; current flow from top to bottom

Flow Direction

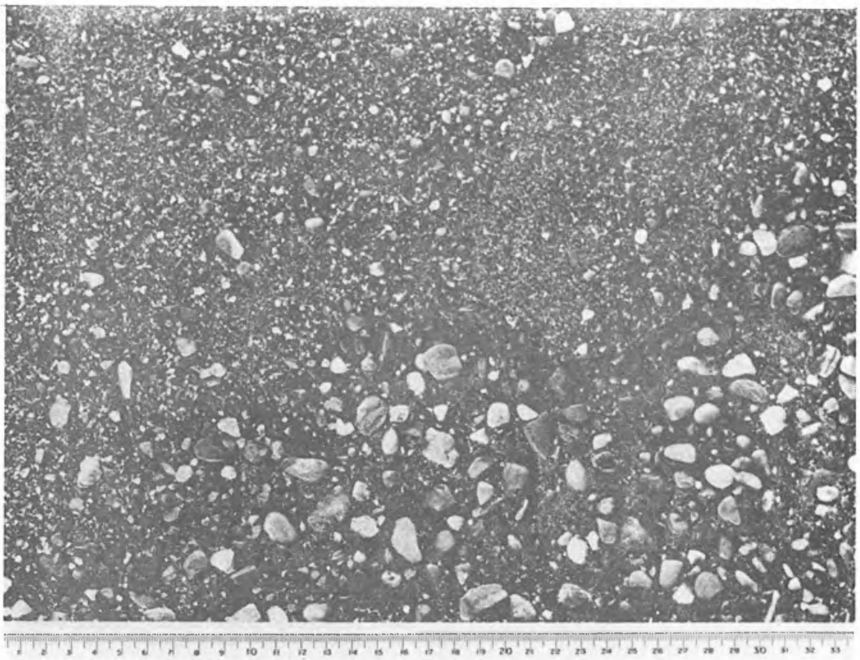

Photograph 3: Front of a ripple; in front of the ripple a partially developed top layer

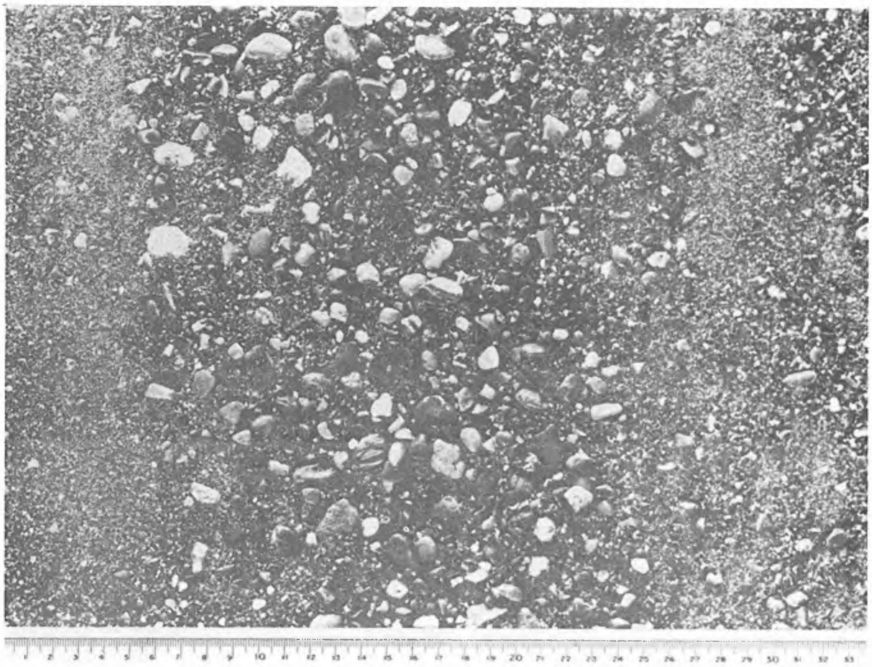

Photograph 4: Sediment transport in longitudinal stripes, as a result of secondary currents. A longitudinal strip is found on the left and right hand side of the figure; in between is the well developed top layer

Flow Direction

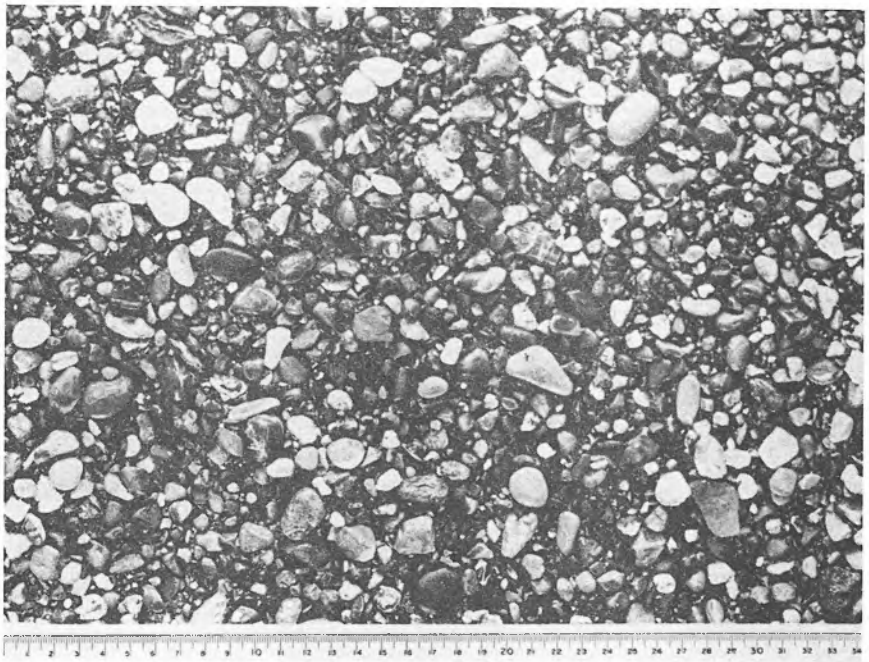

Photograph 5: Completely developed top layer at the end of an experiment

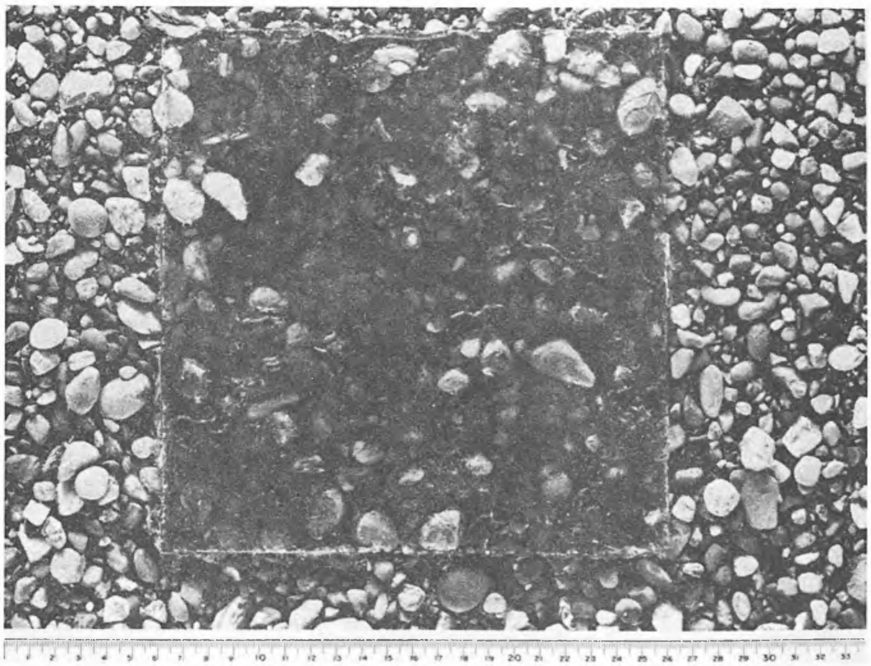

Photograph 6: Top layer after pouring the resin

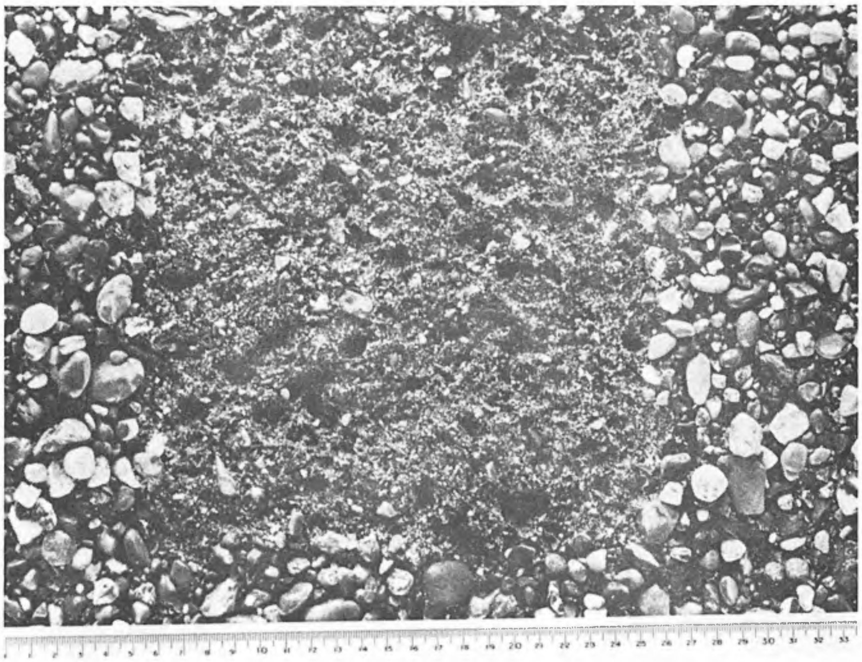

Photograph 7: The bed after removing part of the top layer

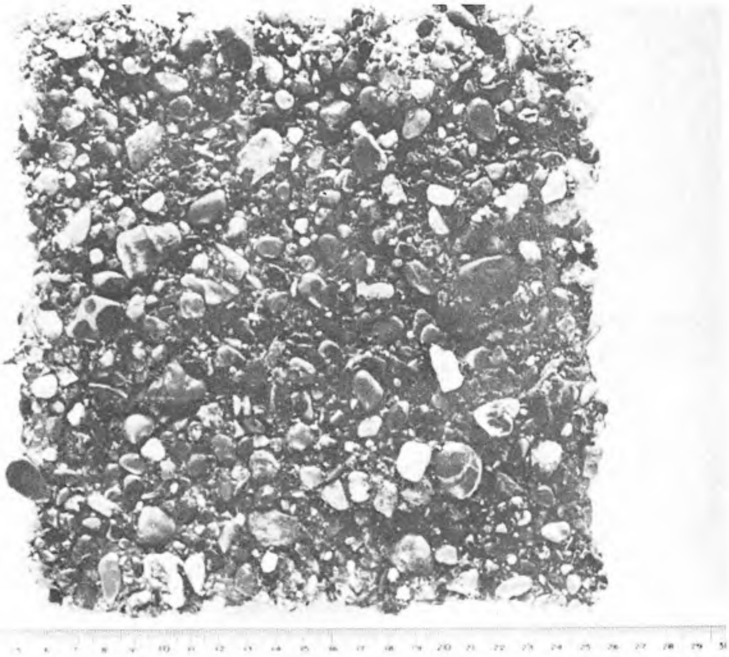

Photograph 8: Bottom view of the resin plate

REFERENCES

(1) CASEY H. - "Ueber Geschiebebewegung" - Mitteilung der Preussischen Versuchsanstalt für Wasserbau und Schiffbau, Heft 19, Berlin 1935

(2) EGIAZAROFF I.V. - "L'Equation Générale du Transport des Alluvions Noncohésives par un Courant Fluide" - VII. Assemblée générale AIHR, Lissabon 1957

(3) EGIAZAROFF I.V. - "Large Range Mixture Sediment Movement and Discharge Shadowing and Self Pavement Effects" - Mitteilung der armenischen Akademie der Wissenschaften, Reihe der technischen Wissenschaften, XVII No. 2 und 3, 1964

(4) EIDGENÖSSISCHES AMT FÜR WASSERWIRTSCHAFT - "Untersuchungen in der Natur über Bettbildung, Geschiebe- und Schwebstofführung" - Mitteilung Nr. 33, Bern 1939

(5) EINSTEIN H.A. - "Der hydraulische oder Profilradius" - Schweizerische Bauzeitung, Band 103 Nr. 8, 1934

(6) EINSTEIN H.A., EL SAMNI EL-S.A. - "Hydrodynamic Forces on a Rough Wall" - Review of Modern Physics 21, 1949

(7) EINSTEIN H.A. - "The Bed-Load Function for Sediment Transportation in Open Channel Flows" - Technical Bulletin No. 1026, U.S. Dep. of Agriculture, Washington D.C., 1950

(8) IWAGAKI Y. - "Hydrodynamical Study on Critical Tractive Force" - Transactions of the Japan Society of Civil Engineering, No. 41, Tokio 1956

(9) KALINSKE A.A. - "Movement of Sediment as Bed-Load in Rivers" - Transactions, American Geophysical Union, Vol. 28 No. 4, 1947

(10) KEULEGAN G.H. - "Laws of Turbulent Flow in Open Channels" - Journal of Research of the National Bureau of Standards, Vol. 21, U.S. Dep. of Commerce, 1938

(11) KRAMER H. - "Modellgeschiebe und Schleppkraft" - Mitteilung der Preussischen Versuchsanstalt für Wasserbau und Schiffbau, Heft 9, Berlin 1932

(12) LANE E.W., CARLSON E.J. - "Some Factors Affecting the Stability of Canals Constructed in Coarse Granular Material" - IAHR-Proceedings Minnesota International Hydraulics Convention, 1953

(13) LIU H.K. - "Mechanics of Sediment-Ripple Formation" - Proceedings of the ASCE, Vol. 83, No. HY 2, 1957

(14) MEYER-PETER E., MÜLLER R. - "Eine Formel zur Berechnung des Geschiebetriebes" - Schweizerische Bauzeitung, 67. Jg. Nr. 3, 1949

(15) NIZERY A., BRANDEAU G. - "Variation de la Granulométrie de Charriage dans une Section de Rivière" - IAHR-Proceedings Minnesota International Hydraulics Convention, 1953

(16) SCHLICHTING H. - "Grenzschichttheorie" - Karlsruhe 1958

(17) SHIELDS A. - "Anwendung der Aehnlichkeitsmechanik und der Turbulenzforschung auf die Geschiebebewegung" - Mitteilung der Preussischen Versuchsanstalt für Wasserbau und Schiffbau, Heft 26, Berlin 1936

(18) VANONI V.A. - "Measurements of Critical Shear Stress for Entraining Fine Sediments in a Boundary Layer" - Report No. KH-R-7, W.M. Keck Laboratory of Hydraulics and Water Resources, California Institute of Technology, Pasadena 1964

(19) WHITE C.M. - "The Equilibrium of Grains on the Bed of a Stream" - Proceedings of the Royal Society Series A, Vol. 174, 1940

(20) YALIN M.S. - "An Expression for Bed-Load Transportation" - Proceedings of the ASCE, Vol. 89, No. HY 3, 1963